Electron-positron annihilation cross section near the new threshold

John Kogut*
Laboratory of Nuclear Studies, Cornell University, Ithaca, New York 14853

Leonard Susskind†
Belfer Graduate School of Science, Yeshiva University, New York, New York 10033
and Tel Aviv University, Ramat Aviv, Israel

(Received 9 June 1975)

Heavy-quark models of the new narrow resonances are presented. The relative heaviness of the assumed new quarks suggests applying the adiabatic approximation familiar from molecular physics here. This approach provides partial justification for the use of potential models to describe the new resonances. Vacuum polarization plays an important role in determining the shape of the adiabatic potential. Model calculations of the $\psi''(4.1)$ are presented. Agreement with experiment is good. A coupled-channel formulation of the narrow resonances and the new threshold is presented. The resulting coupled-channel Schrödinger equations can be solved iteratively. The lowest-order approximation reproduces the adiabatic picture and higher-order corrections are calculable. Several coupled-channel models are analyzed numerically and qualitatively. Although detailed numerical results are model-dependent, certain trends occur. We estimate that the radiative decays of the $\psi'(3.7)$ should be less important than is indicated by naive-pure-quark-model calculations. In addition, the $\psi'(3.7)$ is not a simple two-quark state but has considerable charm-anticharm-meson content. The leptonic widths of the $\psi(3.1)$ and $\psi'(3.7)$ are computed and good agreement with experiment is found. Corrections to the adiabatic-potential-model approximation to $R(Q^2) = \sigma(e^+e^- \to \text{hadrons})/\sigma(e^+e^- \to \mu^+\mu^-)$ above threshold are computed. If the coupled-channel model uses the SU(4) charm scheme, then D*'s are expected to outnumber D's by a wide margin above threshold. The potential-model calculations of $R(Q^2)$ which accept the conventional SU(4) scheme are systematically below the data for $E_{\text{c.m.}} \gtrsim 4.6$–$4.8$ GeV. By adding the contribution of a heavy lepton with mass 2.3–2.4 GeV to the four-quark prediction, a curve of R vs $E_{\text{c.m.}}$ which is in good agreement with the data over the entire energy range occurs.

I. INTRODUCTION

The discovery of two narrow resonances[1] of masses 3.1 and 3.7 GeV, respectively, and the large value of $R = \sigma(e^+e^- \to \text{hadrons})/\sigma(ee \to \mu\mu)$ above 4.0 GeV strongly suggest the existence of new, relatively heavy hadronic degrees of freedom.[2] A popular interpretation of the data postulates the existence of one or more heavy quarks which exist in addition to the colored $\mathcal{P}$, $\mathfrak{N}$, and λ. Then the narrow resonances are thought to be S-wave bound states of the heavy quarks. The long lifetimes of these states suggest that the heavy quarks carry a new quantum number which is conserved by strong interactions. This quantum number is often called charm.[3] Charmed hadrons are then defined as bound states of a charmed quark and ordinary quarks, while the new resonances are bound states of a charm-anticharm quark pair. This scheme suggests further that the broad enhancement in R near 4.1 GeV is caused by the existence of a bound state of heavy quarks which lies above the threshold for production of charmed hadrons.

It is the purpose of this article to analyze models of the new resonances and the e^+e^- annihilation cross section above charm hadron threshold. We shall argue that the relative heaviness of the new quark(s) allows one to formulate an adiabatic approximation for the new heavy states in analogy to the Born-Oppenheimer approximation[4] for the hydrogen molecule. A physical picture of considerable simplicity will result. It is hoped that it will be a useful stepping stone towards more realistic phenomenologies of the new states.

Before embarking on dynamical models of the heavy quarks we must first assume their numbers and properties. The simplest charm scheme is the original SU(4) model.[5] It contains a new, isosinglet, charge $\frac{2}{3}$, charm $+1$ quark (the $\mathcal{P}'$) in addition to the $\mathcal{P}$, $\mathfrak{N}$, and λ. This model is particularly impressive theoretically because it was invented long ago to explain the absence of neutral strangeness-changing currents and was reasonably explicit in predicting charmed hadrons of masses in the several GeV range. It is also economical—only one new quark is introduced. However, it is not at all clear that nature is impressed by our histori-

cal bias. However, whenever it is necessary to assume a particular quark scheme in the text we shall base our considerations on the asymptotically free[6] non-Abelian gauge theory of twelve quarks. Then the $\psi(3.1)$ is viewed as a $1\,^3S$ $\mathcal{C}'\mathcal{C}'$ bound state and the $\psi'(3.7)$ is the first radial excitation of that state. The broad $\psi''(4.1)$ is the would-be $3S$ state which lies above charmed particle threshold. It is a fact that the mass spacings between the ψ, ψ', and ψ'' are understandable in terms of forces of a conventional strength.[7,8] This fact motivates our assumption that the ψ' and ψ'' are radial excitations.

However, these assignments for the ψ's and the SU(4) scheme in general are already in serious experimental trouble. First, R is too large at $Q^2 \approx 50$ GeV^2 to be understood simply by the SU(4) scheme.[9,10] Perhaps several quarks with masses of about 2 GeV must be introduced to explain the new data.[11] But if that is done, the simple assignments for ψ, ψ', and ψ'' may not survive. Our adiabatic potential model calculations of R lie below the data for $E_{\text{c.m.}} \gtrsim 4.6$–$5.0$ GeV if we use the SU(4) scheme. However, it is noted that if a heavy lepton of mass 2.3–2.4 GeV exists, then its contribution to R brings the model calculations into good agreement with the data. The existence of a heavy lepton will be easily confirmed or refuted experimentally. Second, no charmed hadrons have been unambiguously identified in the final states of e^+e^- annihilation.[12] The recent experimental searches have not yet ruled out the SU(4) scheme but may do so in the very near future. Third, a discrepancy of a more model-dependent nature exists. Most models of the charmonium states assume that a quark-confining potential acts between heavy quarks.[7,8,13] This potential insures that $2P$ states lie somewhere between the ψ and the ψ'. For example, the many authors of Ref. 8 tried

$$V(r) = -\frac{\alpha_s}{r}\left[1 - (r/a)^2\right], \quad \alpha_s \approx 0.2, \quad a \approx 0.2 \text{ fm}. \tag{1.1}$$

The first term in Eq. (1.1) was motivated by asymptotic freedom and the second term by the hope of quark confinement.[14] In such a potential the $2P$ states lay 230 MeV below the $2S$ state, so one expected copious monochromatic γ rays coming from the electromagnetic transitions of the ψ' into the $2P$ levels. These spectral lines have not been observed.[15] We shall see that coupled-channel dynamics to be described in the text lead to smaller $2P$-$2S$ mass differences. Since the transition rate for $2S \to 2P + \gamma$ depends on the third power of the photon energy, the discrepancy between theory and experiment is significantly reduced and possibly eliminated. The quark models based on Eq. (1.1) also predicted leptonic widths of the ψ and ψ' which were at odds with experiment. However, the same coupled-channel effects which reduce the $2P$-$2S$ mass difference also lead to new leptonic widths which agree with the data.

Some of our results, both qualitative and quantitative, follow, fortunately, just from the existence of heavy quarks and a new threshold near 4.0 GeV. We shall point these out in the text. One hopes that something of what will be said in the following pages will survive the turmoil of the next six months.

The text is organized as follows. We begin by reviewing the Born-Oppenheimer approximation in the context of a many-body problem and its application, introduced in Ref. 16, to the heavy-quark problem. This approach provides some justification for the use of potential models in heavy-quark phenomenology. Our comments, which are introduced in an intuitive fashion, are then illustrated in two models of quark confinement. These field-theory calculations produce adiabatic potentials which act between heavy quarks. Although the models are field theories in one space dimension, they embody quark confinement in models with a high-mass charmed hadron threshold. The lessons learned from these exercises are then incorporated into a coupled-channel model of the new resonances and the new threshold in $(3+1)$ dimensions. These models lead to results which are suggestive of the data. In most cases, in fact, quantitative success can be claimed. Some discrepancies in simpler potential models constructed without knowledge of the new threshold are removed in a fairly natural fashion. Although the realism of the adiabatic approximation to the problem at hand can be challenged, it does lead to numerical results which are understandable in simple physical terms. The coupled-channel models also make new predictions. In general, the nearness of the new threshold causes a substantial part of the $\psi'(3.7)$ wave function to consist of charm-anticharm hadrons. A particular model illustrated in detail suggests that $D^*\bar{D}^*$ production is responsible for the bulk of the 4.1-GeV enhancement in R. Another curious prediction is the possibility that $\sigma(e^+e^- \to \text{hadrons})$ possesses narrow, but small "glitches" in the vicinity of 4.6 or 4.9 GeV. Here the term "glitch" means a variation in R by a factor of 2–5 in an energy region of width 20–50 keV. These relatively small effects are residues of quark confinement which survive, at least in the simple models presented here, the coupled-channel dynamics.

All of our model calculations of $R(Q^2)$ based on the conventional four-quark scheme fail to fit the data for $E_{\text{c.m.}} \gtrsim 4.6$ GeV. However, the addition of

a heavy lepton of mass 2.3–2.4 GeV to $R(Q^2)$ produces good agreement with the experimental curve over the entire energy range explored to data and it leaves intact the dynamical models of ψ, ψ', and ψ'' discussed here. Tests of this simple (cheap) solution to a serious problem afflicting the four-quark scheme are discussed briefly.

II. THE ADIABATIC APPROXIMATION

The purpose of this section is to lay the qualitative, intuitive groundwork for later, more precise developments. The problem in principle is a quark field theory consisting of four or more species of colored quarks coupled minimally to non-Abelian gauge fields,

$$\mathcal{L}=\bar{\psi}(i\not{\partial}-m)\psi-g\bar{\psi}\gamma_\mu C^\alpha\psi A_\alpha^\mu-\tfrac{1}{4}F_{\mu\nu}^\alpha F_\alpha^{\mu\nu}\,, \tag{2.1}$$

where C^α are the eight, 3×3 color matrices of SU(3)′ and the rest of the notation is standard.[17] This theory has the virtue of being asymptotically free[6] if the number of quarks is not too large. Complementing this good short-distance behavior is the possibility that the theory is infinitely strongly coupled at large distances in such a way that all color nonsinglet states are eliminated from the physical spectrum.[18] Strong-coupling methods are being developed for these theories to determine if this hope is real.[14] We shall simply assume it here and turn to simpler field theories of confinement in Sec. III in order to test some of the ideas put forward in this section.

For our purposes here we are particularly interested in Eq. (2.1) in the SU(4) model with the idealization that $m_{\mathcal{O}'}\gg m_{\mathcal{O}}$ and $m_{\mathfrak{N}}$. Then bound $\mathcal{O}'\bar{\mathcal{O}}'$ states might be characterized by two distinct time scales, that associated with the light quarks and massless gluons and a second associated with the heavy, slow $\mathcal{O}'$. In some applications it can then prove possible to define an effective potential which acts between the heavy quarks. The idea is that the heavy quarks move slowly on the scale of motion characteristic of the light degrees of freedom. Hence, as the heavy quarks move in their bound state, the light degrees of freedom have sufficient time to readjust their spatial distribution and remain in their ground state. Since the light quarks and gluons are not themselves excited in this process, the energy stored in these fields acts as a potential energy residing between the heavy quarks. Therefore, a "potential" can be defined even though the system contains complicated many-body dynamics supporting it.

This ancient approximation scheme, introduced by Born and Oppenheimer,[4] has had many applications in molecular and solid-state physics. In these cases one can in fact estimate the region of validity of the approximation, and compute low-order correction terms. Let us briefly recall a familiar application of the Born-Oppenheimer method. Consider a crystal and the interaction between the lattice of ions and the electrons.[19] Let $\vec{l}_i$ ($\vec{r}_i$) denote the positions of the ions (electrons). The Hamiltonian of the system reads

$$H=-\sum_j\frac{\hbar^2}{2M}\frac{\partial^2}{\partial\vec{l}_j^{\,2}}-\sum_i\frac{\hbar^2}{2m}\frac{\partial^2}{\partial\vec{r}_i^{\,2}}+\sum_{i<j}\frac{e^2}{|\vec{r}_i-\vec{r}_j|}+V(\{\vec{l}\},\{\vec{r}\})+G(\{\vec{r}\})\,, \tag{2.2}$$

where M (m) is the mass of each ion (electron), V is the ion-electron potential energy, and G is the inter-ion potential energy. Now we exploit the fact that $M\gg m$ and formulate the intuitions stated in the preceding paragraph, by considering a trial eigenfunction of the form

$$\Psi=\psi(\{\vec{l}\},\{\vec{r}\})\,\phi(\{\vec{l}\})\,, \tag{2.3}$$

where ψ is an electronic wave function which is defined as a solution to the Schrödinger equation in a lattice of *immobile* ions,

$$\left[-\sum_i\frac{\hbar^2}{2m}\frac{\partial^2}{\partial\vec{r}_i^{\,2}}+\sum_{i,j}\frac{e^2}{|\vec{r}_i-\vec{r}_j|}+V(\{\vec{l}\},\{\vec{r}\})\right]\psi(\{\vec{l}\},\{\vec{r}\})=E_e(\{\vec{l}\})\,\psi(\{\vec{l}\},\{\vec{r}\})\,. \tag{2.4}$$

Note that the energy of the system of electrons, $E_e(\{l\})$, is now a function of the positions of the ions. Finally, Ψ must be a solution to the full problem,

$$H\Psi=E\Psi\,. \tag{2.5}$$

Substituting Eq. (2.3) here and using Eq. (2.4) gives

$$\left[-\sum_j\frac{\hbar^2}{2M}\frac{\partial^2}{\partial\vec{l}_j^{\,2}}+G(\{\vec{l}\})+E_e(\{\vec{l}\})\right]\Psi=E\Psi\,, \tag{2.6}$$

which is best written in the form

$$\psi\left[-\sum_j\frac{\hbar^2}{2M}\frac{\partial^2}{\partial\vec{l}_j^{\,2}}+E_e(\{\vec{l}\})+G(\{\vec{l}\})\right]\phi(\{\vec{l}\})+(\text{correction terms})=\psi E\phi(\{\vec{l}\})\,. \tag{2.7}$$

The "correction terms" in Eq. (2.7) read

$$C=-\sum_j\frac{\hbar^2}{2M}\frac{\partial\phi}{\partial\vec{l}_j}\cdot\frac{\partial\psi}{\partial\vec{l}_j}+\sum_j\frac{\hbar^2}{2M}\phi\frac{\partial^2\psi}{\partial\vec{l}_j^{\,2}}\,. \tag{2.8}$$

Ignore the correction terms temporarily. Then Eq. (2.7) implies that $\phi(\{\vec{\Gamma}\})$, the wave function of ions, satisfies

$$\left[-\sum_j \frac{\hbar^2}{2M}\frac{\partial^2}{\partial \vec{\Gamma}_j^{\,2}} + E_e(\{\vec{\Gamma}\}) + G(\{\vec{\Gamma}\})\right]\phi(\{\vec{\Gamma}\}) = E\phi(\{\vec{\Gamma}\}), \tag{2.9}$$

This equation means that ϕ is determined by an effective potential which consists of G plus the energy of the electrons E_e computed with the ions fixed at their lattice sites. Thus, Eqs. (2.4) and (2.9) formalize the physical adiabatic picture—the electrons' configuration is determined by the lattice of ions which in turn move in a potential determined by that state of the electrons. Clearly, this approach only makes sense if the characteristic time scale governing electronic motion is much smaller than that governing ionic motion. It is also only a practical method if the electrons reside in their ground state.

The corrections to the adiabatic approximation are contained in Eq. (2.8). A rough estimate of the first term suggests that it is $O((m/M)^{1/2})$ of the terms withheld in the adiabatic approximation.[20] So, if $M \gg m$, the correction terms are indeed small. Physically, these correction terms lead to transitions between electronic states. They record the influence of the motion of the ions upon the electronic state and thus destroy the notion that the electrons can remain in a given state while the ions move slowly.

Another application of the Born-Oppenheimer approximation is the calculation of the spectra of molecules. Particularly suggestive is the treatment of the hydrogen *molecule*. Our treatment of charmonium is analogous with the correspondences.

protons → heavy quarks,

electrons → light quarks,

Coulomb field → massless gluons.

We are supposing that the field theory of Eq. (2.1) generates bound states of heavy quarks with the dominant momentum fluctuations in the states characterized by the light quark mass. Then it is plausible that the Born-Oppenheimer approach is a sensible way to view these states and the nearby continuum charmed states. Most workers feel that $m_{\psi'} \lesssim 2.0\,\mathrm{GeV}$ while $m_\psi \approx 300\,\mathrm{MeV}$, so $m_\psi/m_{\psi'} \approx \frac{1}{6}$ with large uncertainties. Therefore, $m_\psi/m_{\psi'}$ may be a reasonable expansion parameter for certain problems. In the solid-state example, however, the ratio of masses is $m/M \approx 10^{-4}$, so in that case superb quantitative calculations are possible. Furthermore, light-quark excitations, a $\mathcal{P}\bar{\mathcal{P}}$ pair, say, require energies of about 600 MeV. This is not a very large energy on the scale of charmonium physics, so the very notion of an effective potential must have a limited region of validity. In the solid-state application, one could be assured that by working at sufficiently low temperatures the electronic states could not be excited with appreciable probability and the adiabatic assumption—that the electrons readjust to the ionic motion *and* remain in their ground state—proved good. In the application here, we are clearly on much less firm ground, and a much more restricted set of problems will be accessible to us. We will discuss the corrections to our physical picture further throughout the text.

III. QUARK CONFINEMENT MODELS WITH FIXED SOURCES

The first step in an adiabatic calculation is the determination of the effective potential acting between the immobile degrees of freedom. In the example sketched in Sec. II, this quantity was $G(\{\vec{\Gamma}\}) + E_e(\{\vec{\Gamma}\})$, where $G(\{\vec{\Gamma}\})$ is the ion-ion potential in the absence of the electrons and $E_e(\{\vec{\Gamma}\})$ is the energy of the electrons themselves. Clearly, to obtain $E_e(\{\vec{\Gamma}\})$ precisely one must solve a many-body problem. In formulating the adiabatic approximation for the theory of heavy quarks, light quarks, and massless gluons it is profitable to think in lines analogous to this many-body problem. In correspondence to $G(\{\vec{\Gamma}\})$ we compute the potential between heavy quarks treating the gauge field exactly but ignoring the light quarks. Finally, the light quarks are treated as quantized dynamical fields and the field-theoretic analog of $E_e(\{\vec{\Gamma}\})$ is obtained.

It is presently beyond a field theorist's powers to obtain the analogs of G and E_e from first principles [the $\mathcal{L}$ in Eq. (2.1), say]. Instead, we shall have to resort to models and prayer (not necessarily in that order). The models we shall consider are two field theories of confinement: the original Schwinger model[21] and the Schwinger model with a nonzero fermion mass.[22] These are theories in $(1+1)$ dimension where confinement is a natural phenomenon. The prayer is that confinement occurs in properly constructed $(3+1)$-dimensional gauge theories and that the gross features of confinement are similar to the $(1+1)$-dimensional models. There are reasons to be optimistic here.[14] Assuming this, we can proceed to identify G and E_e. The analog of G is the unscreened potential between the heavy quarks. At short distances G should be

$$G(r) \sim \frac{g^2}{r}\,\frac{1}{\ln(r_0/r)}, \quad r \ll r_0 \tag{3.1}$$

in accord with the asymptotic freedom[6] of the pure Yang-Mills theory in (3+1) dimensions. At larger distances G presumably grows linearly with r,[14]

$$G(r) \sim \kappa r, \quad r \gg r_0 . \tag{3.2}$$

Of course, $G(r)$ itself is *not* the physically relevant potential which acts between the $\mathcal{P}'\bar{\mathcal{P}}'$ pair—we must also introduce the light quarks into the picture. For a given separation between the heavy quarks, the light-quark field will assume a spatial distribution which minimizes the energy of the system. This effect is particularly significant at large $\mathcal{P}'\bar{\mathcal{P}}'$ separation where the energy stored in the gauge field between the heavy quarks is large. It has been argued that the light quarks will screen the long-range force, thereby reducing the energy of the system and insuring that only color singlet states are physical.[23] Granting this, we can rough out the expected effect of the light quarks on the potential between the $\mathcal{P}'\bar{\mathcal{P}}'$ pair. At small separations, the problem is amenable to perturbation theory. If the number of species of light quarks is not too large, then

$$G+E \sim \text{const} \times \frac{g^2}{r} \frac{1}{\ln(r_0/r)}, \tag{3.3}$$

where only the over-all strength of the potential is changed from Eq. (3.1).[6] As r is increased the potential tends to rise faster than the Coulomb potential, because the Yang-Mills electric field tends to form a tubelike configuration between the heavy quarks.[14] However, the long-range force can be screened now by the appearance of a pair of light quarks in the growing potential. It is energetically favorable for each light quark to pair off with the appropriate heavy quark so that two color singlet states result. There is no long-range force between the color singlet states (a charmed and an anticharmed meson) so one expects, on the basis of typical hadronic physics, that

$$G+E \sim e^{-m|r|}, \quad r \text{ large} \tag{3.4}$$

in place of Eq. (3.2). The energy of the $\mathcal{P}'\bar{\mathcal{P}}'$ pair plus the screening cloud of light quarks has become the sum of the masses of the two charmed mesons as $r \to \infty$. The physically relevant potential, Eq. (3.3) and Eq. (3.4), is sketched in Fig. 1.

A few comments concerning Eqs. (3.3) and (3.4) and the curve in Fig. 1 are in order. The short-distance part of the potential in Fig. 1 acts between the heavy quarks. It is logarithmically softer than a Coulomb potential for $r < r_0$, but grows somewhat faster for $r \gtrsim r_0$. As discussed before Eq. (3.4) the long-range piece of the potential can be thought of as acting between charmed mesons. The ionization point of the potential in Fig. 1 signals charm meson production. However, in the adiabatic approximation the long-range piece of the potential equals the potential acting between the heavy quarks in that state. To see this, recall that to calculate the potential between the charmed mesons one would imagine a virtual displacement $\delta\vec{r}$ of both the heavy and light quark composing one of the charmed mesons. The change in energy incurred by such a virtual displacement is the potential energy change. However, to calculate the potential acting between the heavy quarks one would give a virtual displacement $\delta\vec{r}$ only to a heavy quark and leave its accompanying light quark unmoved. The difference in energy required in these two different virtual displacements is suppressed by a power of $m_{\mathcal{P}}/m_{\mathcal{P}'}$. The reason is that the difference in the electronic wave function in one virtual displacement and the other reads $\partial\psi/\partial\vec{\Gamma}$ in the notation of Sec. II. This gradient is the same as those appearing in the correction term in Eq. (2.8). This gradient records the sensitivity of the electronic state to changes in the positions of the ions. Clearly, it is the premise of the adiabatic approximation that this gradient is small. Detailed analyses of individual applications of the adiabatic method bear this out and give, in general, that this gradient is suppressed by a factor of $(m_{\mathcal{P}}/m_{\mathcal{P}'})^{1/2}$ compared to the terms kept in the approximation scheme. In short, the long-range piece of the potential in Fig. 1 is, to good approximation, the potential which acts between the heavy quarks in the lowest-energy state of the system at that separation distance.

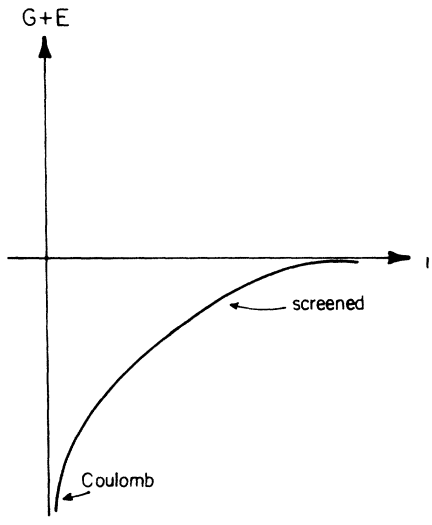

FIG. 1. The adiabatic potential between heavy quarks.

It may be instructive to compare this physical system to the Born-Oppenheimer discussion of the hydrogen molecule.[20] For small proton-proton separation, the interproton potential is essentially unaffected by the two electrons which are smeared over a relatively large volume. As the protons are adiabatically separated, however, it is energetically favorable for the electrons to pair up with each proton to make two hydrogen atoms since the energy of a free proton and a free electron exceeds that of one neutral hydrogen atom. So, at large proton-proton separation the interproton Coulomb force is completely screened and all that remains in the Van der Waals force acting between neutral atoms.

Finally, after this lengthy introduction, consider the calculation of the adiabatic potential between fixed sources in (1+1)-dimensional theories of confinement. Since these theories have been discussed at length elsewhere,[21-23] we shall be brief and to the point. In the absence of external sources the vector current of the Schwinger model satisfies the free Klein-Gordon equation

$$(\Box + m^2) j_\mu = 0, \quad j_\mu = \bar{\psi} \gamma_\mu \psi \tag{3.5}$$

where $m^2 = g^2/\pi$ and g is the analog of the (strong) electric charge. In the presence of an external current, Eq. (3.5) becomes[23]

$$(\Box + m^2) j_\mu = -m^2 j_\mu^{\text{ext}}, \tag{3.6}$$

where j_μ^{ext} will be chosen to represent a fixed charge of $+1$ at $r = a$ and -1 at $r = -a$.[24] Since both currents j_μ and j_μ^{ext} are conserved, the (1+1) dimensionality of the theory insures that they can be written as the curls of scalar fields,

$$j_\mu = \frac{1}{\sqrt{\pi}} \epsilon_{\mu\nu} \partial^\nu \phi, \quad j_\mu^{\text{ext}} = \frac{1}{\sqrt{\pi}} \epsilon_{\mu\nu} \partial^\nu \phi^{\text{ext}}. \tag{3.7}$$

Therefore, Eq. (3.6) simplifies to

$$(\Box + m^2) \phi = -m^2 \phi^{\text{ext}}. \tag{3.8}$$

Since the external current is

$$j_{\text{ext}}^\mu = \delta_{0\mu} [\delta(x+a) - \delta(x-a)] \tag{3.9}$$

the external field is

$$\phi^{\text{ext}} = -\sqrt{\pi}\, \theta(a - |x|), \tag{3.10}$$

so Eq. (3.8) becomes

$$(\Box + m^2) \phi = -\sqrt{\pi}\, m^2 \theta(a - |x|). \tag{3.11}$$

We finally wish to calculate the energy in the system with the sources a distance $2a$ apart. Rewriting the Hamiltonian of the Schwinger model in terms of ϕ gives

$$H = \frac{1}{2} \int dx \left[\dot{\phi}^2 + \left(\frac{\partial \phi}{\partial x} \right)^2 + \frac{g^2}{\pi} (\phi + \phi^{\text{ext}})^2 \right]. \tag{3.12}$$

Interpreting ϕ as a canonical scalar field, one easily checks that the Heisenberg equations of motion for Eq. (3.12) yield the equation of motion, Eq. (3.8). A complete derivation of Eq. (3.12) proves that the Schwinger model confines quarks—its only finite-energy excitations are neutral, free, massive mesons.[25]

In the static limit Eqs. (3.11) and (3.12) become

$$\left(-\frac{d^2}{dx^2} + m^2 \right) \phi = -\sqrt{\pi}\, m^2 \theta(a - |x|), \tag{3.13}$$

$$E(2a) = \tfrac{1}{2} \int dx [\partial\phi/\partial x)^2 + m^2 (\phi + \phi^{\text{ext}})^2]. \tag{3.14}$$

Solving Eq. (3.13) for the scalar field gives

$$\phi = -\frac{\sqrt{\pi}}{2} m \int_{-a}^{+a} e^{-m|x-x'|}\, dx'. \tag{3.15}$$

Finally, the adiabatic energy can be evaluated,

$$E(2a) = -\tfrac{1}{2} \pi m (e^{-2ma} - 1). \tag{3.16}$$

Thus, $E(2a)$ is a *short*-range potential—the underlying massless-quark field has screened the long-range electrostatic potential completely. In the language of Sec. II the function G is a linearly rising potential—just Coulomb's law in (1+1) dimension. However, the adiabatic potential $G + E_e$ is short range because the massless fermions react to the long-range force and screen it out of the finite-energy sector of the theory. Note that for $2a \ll 1/m$,

$$E(2a) \approx -\frac{\pi}{2} m(-2ma) + \cdots = g^2 a + \cdots, \tag{3.17}$$

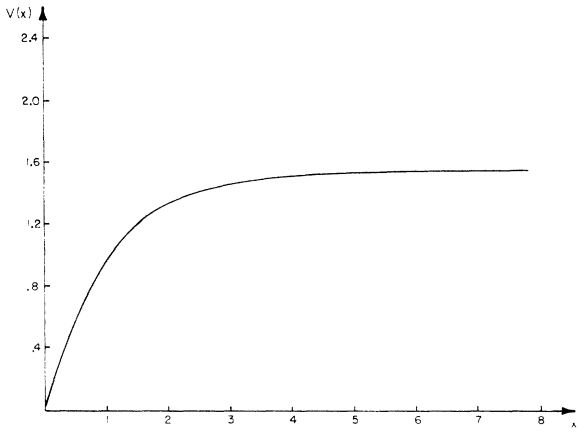

FIG. 2. The adiabatic potential between fixed sources in the Schwinger model. The mass $m = g/\sqrt{\pi}$ was chosen to be 1, and distances are then measured in these units. x is the distance between the oppositely charged (color) fixed sources.

which states that for these short distances the heavy quark interact via a force g^2. This is the only remnant of the Coulomb force. As $2a \to \infty$, E approaches $\frac{1}{2}\pi m = \frac{1}{2}\sqrt{\pi}\, g$, which represents the ionization potential for two neutral bound states, each containing a heavy quark. The adiabatic potential Eq. (3.16) is graphed in Fig. 2.

There are several lessons to learn from this exercise. It should serve as a warning to quark-model builders who employ a linearly rising potential to calculate the meson spectrum. Even if the linearly rising potential is the unscreened force law between quarks in (3+1) dimensions, it does not necessarily show up simply in the spectrum of physical states.

This example has the virtue that the field-theoretic analog of $G+E_e$ could be obtained exactly, i.e., the light-quark-gluon sector of the theory is soluble. Equations (3.15) and (3.16), although written in informal notation, are the exact ground-state expectation values of the quantized field ϕ and the Hamiltonian, respectively.

Now turn to a similar exercise in the massive Schwinger model to investigate the sensitivity of the above results to the bare fermion mass μ. Some of the effects of nonzero μ can be anticipated from the following considerations. When the two static sources are slowly separated, energy appears in the unscreened Coulomb force between them. This force is screened when a pair of light quarks is created from that field. If $\mu = 0$ the screening occurs with no effort. But if $\mu \neq 0$, the energy in the Coulomb field must rise above $\sim 2\mu$ before the screening is very effective. Therefore, one might expect the long-range field to play a more interesting role in determining the mass spectrum and the adiabatic potential if $\mu \neq 0$.

Insert the static sources, Eq. (3.9), into the massive Schwinger model. The theory is again most simply analyzed in terms of the scalar field ϕ (Coulomb gauge). To proceed, we need the $\mu \neq 0$ analogs of Eqs. (3.8) and (3.12), i.e., we need expressions for the neutral composite operator $\mu\bar{\psi}\psi$ in terms of ϕ. This problem has been discussed in Ref. 22, with the result

$$\mu{:}\bar{\psi}\psi{:} = K\cos(2\sqrt{\pi}\,\phi)\,, \tag{3.18}$$

where $K = \mu m e^{\gamma}/2\pi$, γ = Euler-Macaroni constant. The generalizations of Eqs. (3.8) and (3.12) become

$$(\Box + m^2)\phi + 2\sqrt{\pi}\,K\sin(2\sqrt{\pi}\,\phi) = -m^2\phi^{\text{ext}} \tag{3.19}$$

and

$$H = \frac{1}{2}\int\left[\dot{\phi}^2 + \left(\frac{\partial\phi}{\partial x}\right)^2 + \frac{g^2}{\pi}(\phi+\phi^{\text{ext}})^2 - 2K\cos(2\sqrt{\pi}\,\phi)\right]. \tag{3.20}$$

Choosing ϕ^{ext} as before, one can analyze the static limit of these expressions. Unfortunately, we cannot solve the quantized massive Schwinger model without sources because of the presence of the nonlinear term $\cos(2\sqrt{\pi}\,\phi)$ in the Hamiltonian. Therefore, we shall restrict our attention to those cases where the nonlinearities are small so a classical analysis of these equations is a good approximation. This means we must take μ small compared to $m = g/\sqrt{\pi}$. One can show in fact that for μ sufficiently small the one-loop correction to the adiabatic potential is small (of order μ^2) and well behaved. It is also known that mass perturbation theory for the massive Schwinger model converges for μ infinitesimal, so the classical calculation is on firm ground.[22,26] The analysis of Eqs. (3.19) and (3.20) proceeded numerically for several choices of small μ. The resulting adiabatic potentials are shown in Fig. 3(a) and 3(b). We see that by increasing μ, the ionization energy grows and the region over which the potential grows linearly with distance also increases.

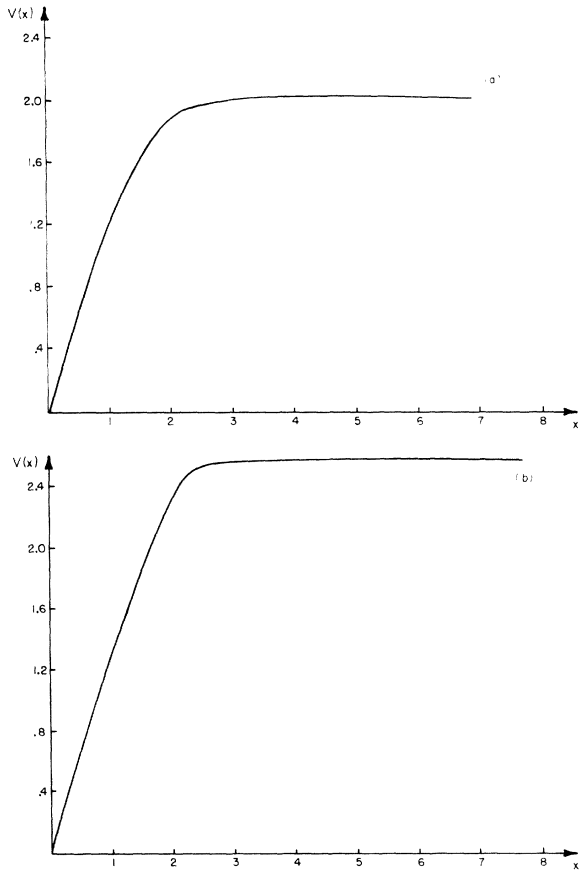

FIG. 3. (a) The adiabatic potential in massive Schwinger model with $m = 1$, $\mu = 0.34$. (b) Same as (a), but $\mu = 0.67$.

These results are in accord with the qualitative arguments sketched above. The curves of Fig. 3 are considerably more interesting than the $\mu = 0$ case. They suggest that the massive Schwinger model has an interesting spectrum (a wedge-shaped potential can bind more states than an exponential).

Now we shall use the adiabatic method and these suggestions from simple models of confinement to discuss $\sigma(e^+e^- \to \text{hadrons})$ in the vicinity of the new threshold.

IV. SIMPLE MODEL CALCULATIONS OF $\sigma(e^+e^- \to \text{hadrons})$

Consider e^+e^- annihilation above but near the threshold for production of charmed hadrons. The virtual timelike photon γ^* decays into a $\mathcal{P}'\bar{\mathcal{P}}'$ pair which slowly separate. The potential (non-Abelian electric flux) grows between them until it is energetically favorable for a pair of light quarks to be created. The light quarks associate with the appropriate heavy quarks such that two charmed hadrons escape to infinity. The total cross section for these events is given by

$$\sigma_{\mathcal{P}'}(Q^2) = \frac{8\pi^2\alpha^2}{3Q^4}\int d^4x\, e^{iq\cdot x}\langle 0|[J_\mu(x), J^\mu(0)]|0\rangle\ , \tag{4.1}$$

where $J_\mu(x)$ is the $\mathcal{P}'$ contribution to the electromagnetic current. Upon inserting a sum over outgoing hadrons into Eq. (4.1), we have

$$\sigma_{\mathcal{P}'}(Q^2) = \frac{8\pi^2\alpha^2}{3Q^4}\sum (2\pi)^4\delta^4(q - p_1 - p_2) \times |\langle 0|J_\mu(0)|H(p_1)\bar{H}(p_2)\rangle|^2\ , \tag{4.2}$$

where $H(p_1)$ is a charmed hadron of momentum p_1 and $\bar{H}(p_2)$ is an anticharmed hadron of momentum p_2. To compute Eq. (4.2) we need the $H\bar{H}$ wave function in the vicinity of the origin. But here, as discussed in the previous section, the outgoing eigenstate of the dynamics is just a $\mathcal{P}'\bar{\mathcal{P}}'$ pair. To couple to the photon, such a pair is in a ^3S state. Furthermore, in the adiabatic approximation in which $m_{\mathcal{P}'} \gg m_{\mathcal{P}}$ and the binding energy of the $\mathcal{P}'$ quark in the charmed hadron is of order $m_{\mathcal{P}}$, which is negligible compared to $m_{\mathcal{P}'}$, the momentum p_1 of the outgoing hadron H is closely approximated by the momentum of the $\mathcal{P}'$ just after creation. Therefore,

$$|\langle 0|J_\mu(0)|H\bar{H}\ \text{out}\rangle|^2 \cong |\bar{u}(p_1, s)\gamma_\mu v(p_2, s)|^2|\psi(0)|^2\ , \tag{4.3}$$

where u, v denote quark spinors and $\psi(0)$ is the wave function at the origin (the amplitude to create the quark pair). Now the sum over final states is trivial—it just reproduces the cross section to produce two free heavy quarks. All the dynamics is contained in the factor $\psi(0)$. Therefore, the $\mathcal{P}'$ quark contribution to $\sigma(Q^2)$ becomes

$$\sigma_{\mathcal{P}'}(Q^2) = \left(\frac{4\pi\alpha^2}{3Q^2}\right)3(\tfrac{2}{3})^2(1 - s_0/s)^{1/2}(1 + s_0/2s) \times |\psi(0)|^2\ , \tag{4.4}$$

where $\frac{1}{2}\sqrt{s_0}$ is the mass of the charmed meson [equal to $m_{\mathcal{P}'} + O(m_{\mathcal{P}})$]. The numerical factors 3 and $(\frac{2}{3})^2$ register the number of $\mathcal{P}'$ quarks (3 colors) and its charge squared. Therefore, the $\mathcal{P}'$-quark contribution to R (call it $R_{\mathcal{P}'}$) reads[16]

$$R_{\mathcal{P}'} = 1.33(1 - s_0/s)^{1/2}(1 + s_0/2s)|\psi(0)|^2\ . \tag{4.5}$$

Several comments concerning Eqs. (4.3) and (4.5) are in order. Note that the heaviness of the $\mathcal{P}'$ quark is *essential* to the factorization noted in Eq. (4.3). The factorization stems from the fact that the act of creation of the $\mathcal{P}'\bar{\mathcal{P}}'$ pair and their eventual evolution into a pair of outgoing charmed hadrons are independent processes. The factorization is guaranteed by the presence of two explicit, very different time scales in the problem. The first is $m_{\mathcal{P}'}^{-1}$, which is the temporal uncertainty in the creation of the heavy quarks. The second is $m_{\mathcal{P}}^{-1}$, which is a measure of the time it takes for the final-state mesons to be formed. In the true adiabatic limit in which $m_{\mathcal{P}'}$ can be held fixed while $m_{\mathcal{P}}$ is infinitesimal, it takes forever for the final-state mesons to be formed. The act of creation can then be clearly separated from the formation of the final state. The cross section is then reasonably calculated as in Eqs. (4.3) and (4.5) just in terms of dynamics which occupies a finite time interval. Thus, this impulse-approximation calculation of the cross section can be deduced as a consequence of the adiabatic theorem if $m_{\mathcal{P}}/m_{\mathcal{P}'}$ is infinitesimal.

Note next that Eqs. (4.3) and (4.5) do *not* apply to the light-quark contributions to $\sigma(Q^2)$ near the low-energy thresholds, $Q^2 \approx m_\rho{}^2$. For light quarks the creation of the $\mathcal{P}\bar{\mathcal{P}}$ pair and their evolution into final-state pions occur on comparable time scales. Then an impulse approximation, the factorization of Eq. (4.3), is not a good approximation.

A final word about Eq. (4.3). In the impulse approximation the cross section is determined by heavy-quark kinematics and the value of the wave function at the origin. Thus, an S-wave phase-space factor occurs in Eq. (4.5) although the hadrons making up the final state may be in an $L = 1$ state. This will be the case in the SU(4) model, where the final state will be composed primarily of $D\bar{D}$, $\bar{D}^*D^*$, $F\bar{F}$, etc. pairs. The phase-space

factor for the final hadronic state does not appear in Eq. (4.5) because the evolution of the final state occurs on a much longer time scale than the dynamics which determines the cross section. The pure S-wave phase-space factor is quite sensitive to the adiabatic picture used here, i.e., to the idealization $m_{\mathcal{P}'} \gg m_{\mathcal{P}}$. If one wishes to make a model which is more "realistic," it is necessary to know the details of the final-state dynamics. A study of graphs shows that factorization and the appearance of the S-wave phase-space factor only emerge as $m_{\mathcal{P}}/m_{\mathcal{P}'} \to 0$. The general calculation requires knowledge of the charmed-hadron wave function and the dynamics of vacuum polarization. However, such calculations are constrained by the limiting form of Eq. (4.5), which we will, therefore, accept as an adequate interpolating formula. Given the state of the art and the fact that this idealization produces a simple physical picture of $R_{\mathcal{P}'}$, we feel that our approach is sensible. It will also yield predictions which provide good fits to the data.

A different line of reasoning, which leads to a slightly weaker form of Eq. (4.5) but applies even when $m_{\mathcal{P}}/m_{\mathcal{P}'}$ is not infinitesimal, can be constructed. Consider the massive Schwinger model and Fig. 3. In this model and in those to be presented in Sec. V the heavy quarks can be separated a certain distance D before vacuum polarization effects begin to convert the state into two outgoing hadrons. Consider the e^+e^- annihilation cross section averaged over energies ΔE, i.e.,

$$\bar{\sigma}(E) = \frac{1}{\Delta E} \int_E^{E+\Delta E} \sigma(E)\, dE \,.$$

A space-time analysis of this quantity shows that it is determined by distances less than $1/\Delta E$. If we choose $\Delta E \approx 1/D$, then the calculation of $\bar{\sigma}(E)$ involves only the physics of a pair of heavy quarks being created in a small volume $1/m_{\mathcal{P}'}$ and propagating in a smooth potential out to distances $\approx D$. Thus, the calculation of $\bar{\sigma}(E)$ gives us Eq. (4.4) with the understanding that a smearing over energies $\approx 1/D$ must be done. (In the models of Sec. V $1/D \approx m_\pi$, a small energy.) From this point of view it follows that our calculations of $R_{\mathcal{P}'}$ may not be trustworthy point by point, but should be accurate in their average features (such as the area under prominent bumps or the presence of dips).

We now turn to several simple model calculations of $R_{\mathcal{P}'}$. To evaluate Eq. (4.5) we need $\psi(0)$ computed in an adiabatic potential adjusted to bind a 1S state and its first radial excitation. Furthermore, we must choose the position of the charmed-meson threshold. In accordance with a host of recent arguments[27] we choose the threshold to lie in the vicinity of $E_{\text{c.m.}} = 3.8$–4.0 GeV. A simple motivation for this range of values was provided by Eichten *et al.*,[7] who, in order to obtain a sensible nonrelativistic bound-state model of the $\psi(3.1)$ and $\psi'(3.7)$ with a potential of the form

$$V(r) = -\frac{\alpha_s}{r}\left[1 - (r/a)^2\right], \tag{1.1}$$

chose $\alpha_s = 0.2$, $a = 0.2$ fm, and $m_{\mathcal{P}'} = 1.6$ GeV. With this mass of the $\mathcal{P}'$ quark, one then expects charmed mesons with a mass $m_D \approx m_{\mathcal{P}'} + m_{\mathcal{P}}$ $\approx 1.6 + .30 \cong 1.90$ GeV according to the naive additive quark model.

As a first example consider a wedge-shaped potential as suggested by the massive Schwinger model. In cases where the edge of the wedge is sharp,

$$\begin{aligned} V(r) &= ar - b, \quad r < b/a \\ V(r) &= 0, \quad r > b/a \end{aligned} \tag{4.6}$$

the wave function at the origin $\psi(0)$ can be computed in terms of Airy functions.[28] Instead of dwelling on the routine calculations, we turn directly to graphs of $\psi(0)$ and $R_{\mathcal{P}'}$ itself. These graphs were also obtained by solving the Schrödinger equation numerically. In computing $R_{\mathcal{P}'}$, one must obtain the wave function $\psi(r)$ with the proper continuum normalization of unit flux at spatial infinity. The computer calculations were checked against the analytic solution for $\psi(0)$ in terms of Airy functions. The comparison showed that the numerical integration routine (which was also used in more ambitious calculations, to be described in later sections) of the Schrödinger differential equation was accurate to better than 1 part in 10^4. A trivial check of the over-all normalization of the calculations is afforded by observing that numerically $R_{\mathcal{P}'} \to \frac{4}{3}$ as $Q^2 \to \infty$, in

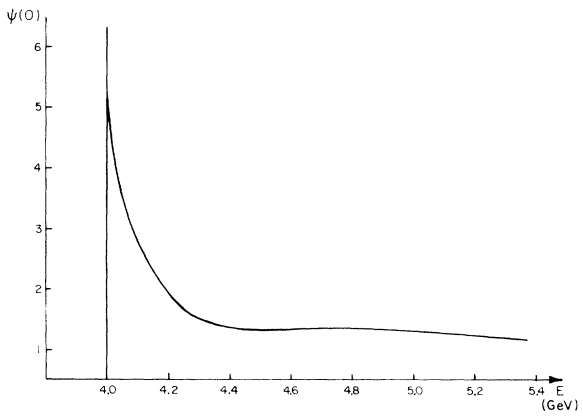

FIG. 4. The amplitude $\psi(0)$ as a function of $E_{\text{c.m.}}$ computed for the wedge potential, $a = 0.25$ GeV^2 and $b = 1.75$ GeV.

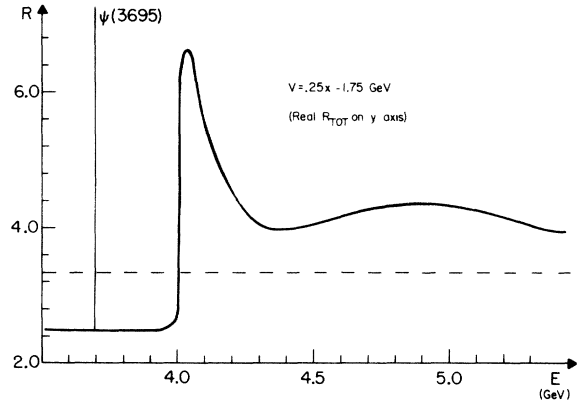

FIG. 5. R as a function of $E_{\text{c.m.}}$ computed for the same potential as in Fig. 4.

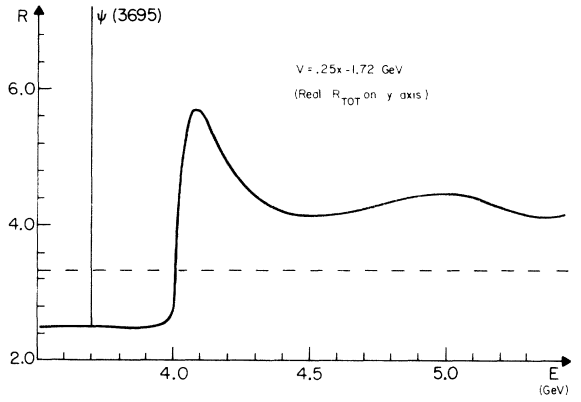

FIG. 7. Same as Fig. 5 except $b = 1.72$ GeV.

agreement with quark counting. In Figs. 4–7 we plot $\psi(0)$ and $R = R_{\phi'} + 2.5$ for the choices $a = 0.25$, $b = 1.75$ and $a = 0.25$, $b = 1.72$ (GeV units everywhere). We choose the sum $R_{\phi'} + 2.5$ since 2.5 is presumably the light-quark contribution to the total R in this energy region. The value 2.5 is read off the SPEAR data[2] just before the new threshold. The value for "a" insures that the energy difference between the $1S$ and $2S$ bound states of this potential is 0.60 GeV and the values for "b" place the threshold in the desired region. Note that these parameters imply that the range of the potential is $b/a \approx 1.72/0.25 \approx 6.88$ GeV^{-1}. This is roughly m_π^{-1}, which is the conventional measure of the range of strong-interaction forces. Observe from the figures that R possesses an enhancement of width ≈ 300 MeV at $E_{\text{c.m.}} \approx 4.1$ GeV. The low-energy edge of the enhancement is sharper than its high-energy tail. Following this enhancement there is a *dip* at about 4.5 GeV which is followed by a very *broad* and *smaller* enhancement. For very large energies R approaches $3\frac{1}{3}$ from above. This asymptotic value of R is, of course, built

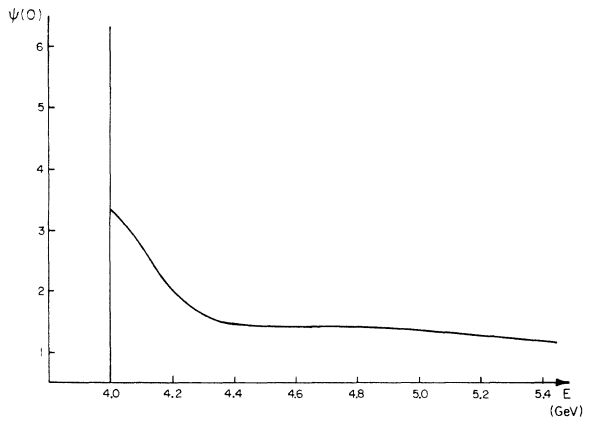

FIG. 6. Same as Fig. 4 except $b = 1.72$ GeV.

into the theory by assuming the SU(4) multiplet of quarks *and* the fact that the forces between quarks are soft and therefore negligible at small distances. It is interesting that the asymptotic value is approached slowly. Even at $E_{\text{c.m.}} \approx 6.0$ GeV, R is still above 3.8. Of course, the approximations underlying the calculation of R (nonrelativistic kinematics, the potential picture) are not reliable this far above threshold. At $E_{\text{c.m.}} \approx 6.0$ GeV it is best to connect our curves to the asymptotic freedom calculations.[29] In fact the connection can be quite smoothly, i.e., asymptotic freedom estimates of R at $E_{\text{c.m.}} \approx 6.0$ GeV also give ≈ 3.8.

The results in Figs. 4–7 can be explained in simple terms. First consider the spectrum of bound S-wave states in the potential

$$V(r) = ar - b\,,$$

which is *not* truncated at $r = b/a$. For the parameters a, b, and $m_{\phi'}$ chosen above, such a potential would bind a $3S$ state of mass ≈ 4.2 GeV. Therefore, when the potential is truncated as in Eq. (4.6), this state lies in the continuum just above the threshold. It is therefore called a virtual bound state.[30] It is not a resonance because the potential of Eq. (4.6) is attractive everywhere. The presence of the virtual bound state causes continuum states just above threshold to be highly distorted with their values at the origin considerably enhanced. This is the dynamical origin of the large value of $\psi(0)$ in the immediate vicinity of threshold. Note that $\psi(0)$ generally decreases as the energy above threshold grows. It has no dramatic structure itself aside from its large value near threshold because the potential of Eq. (4.6) does not possess any resonant states. This will be true of all the examples discussed here and leads us to expect only *one* prominent enhancement in R near 4.1 GeV and no comparable enhancement at higher energies.

The dips and secondary broad enhancements in R result from the following mechanism. To compute R above threshold one multiplies the falling factor $|\psi(0)|^2$ with the phase-space factor $(1-s_0/s)^{1/2}(1+s_0/2s)$ which vanishes at threshold and approaches unity as $s\to\infty$. The result of multiplying these two factors, one which falls and the second which rises, are the curves with bumps shown in Figs. 5 and 7. Thus, in the adiabatic picture the dip which follows the $\psi''(4.1)$ is mostly a kinematic effect.

Let us now repeat these calculations for a more interesting adiabatic potential. It has been argued on the basis of asymptotic freedom that the short-distance forces acting between heavy quarks should be slightly softer than Coulombic forces. Following Eichten *et al.*,[7] this suggests that we consider a potential of the form

$$V(r)=-\frac{\alpha_s}{r}[1-(r/a)^2]-V_0, \quad r\lesssim a^2V_0/\alpha_s \tag{4.7}$$

$V(r)\to 0$ smoothly as $r\to\infty$,

with the parameters α_s, a, V_0, and $m_{\varphi'}$ chosen such that (1) the threshold lies in the vicinity of 3.8–4.0 GeV, (2) the potential binds a $2S$ and a $1S$ states with a mass difference of 600 MeV, (3) α_s lies in the range 0.2–0.3 in accordance with asymptotic freedom calculations,[31] and (4) "$\alpha_s a^2$" is constrained to be $\approx(2\pi)^{-1}$ as suggested by the string model.[32] A typical set of parameters is $\alpha_s=0.19$, $a=0.92$ GeV^{-1}, $m_{\varphi'}=1.6$ GeV, and $V_0=1.55$ GeV. The resulting potential is shown in Fig. 8. $\psi(0)$ was then obtained numerically as a function of the energy above threshold for values of V_0 which were varied between 1.4 and 1.6 GeV in order to determine the sensitivity of the results to the precise position of the threshold. A typical curve of R which results is shown in Fig. 9. Note that the values of R in Fig. 9 at energies above the $\psi''(4.1)$ lie roughly $\frac{1}{4}$ unit *above* those values of R calculated in a potential which omits the Coulomb piece. This effect is expected on rather general grounds. Recall that $\sigma(e^+e^-\to\text{hadrons})$ is determined for asymptotic Q^2 ($Q^2\gg m_{\varphi'}{}^2$, for example) by the behavior of the matrix elements $\langle 0|J_\mu(x)J^\mu(0)|0\rangle$ at short distances, i.e., $x_\mu\approx 1/(Q^2)^{1/2}$. But at distances of order $(m_{\varphi'})^{-1}$ and less, the potential in Eq. (4.7) generates considerable attraction between the heavy quarks compared to the smooth potential of Eq. (4.6). We finally note that the rate of decrease of R with increasing energy is also *slower* in this example. In fact, R is roughly 4.2 at $E_{\text{c.m.}}=6.0$ GeV. Of course, the model is not reliable this far above threshold, but it is suggestive of the possibility that the asymptotic region may lie at higher energies than simple perturbative asymptotic-freedom calculations suggest.

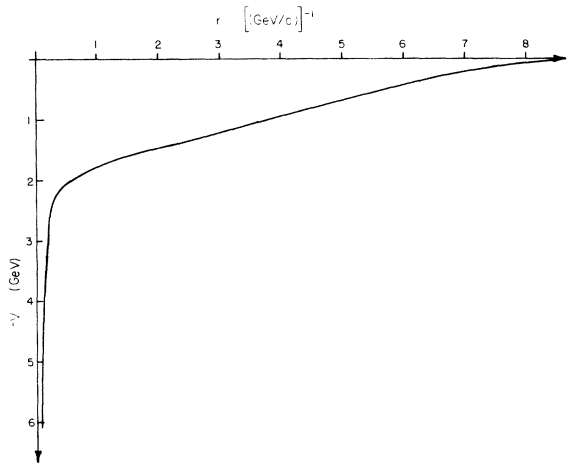

FIG. 8. Potential of Eq. (4.7) with $\alpha_s=0.20$, $a=0.922$ GeV^{-1}, $V_0=1.84$ GeV.

V. COUPLED-CHANNEL MODELS

It proves possible to place the naive considerations of the previous section on firmer ground. In this section we shall define a coupled-channel model of the new resonances and the continuum of charmed hadrons. We shall also solve it approximately in some simple cases. In so doing, a systematic expansion of the solution of the problem will be obtained whose zeroth-order term is the simplest adiabatic approximation.

The basic physical picture of the process $\gamma^*\to\mathcal{P}'\bar{\mathcal{P}}'\to H\bar{H}$ discussed in the previous sections stated that the pair of heavy quarks evolve into the outgoing state of mesons when a pair of light quarks is created out of the vacuum. We can formulate this in the context of a multicomponent Schrödinger equation. Let ψ_j^i denote the wave function for a $\mathcal{P}'$ with spin index i and a $\bar{\mathcal{P}}'$ with spin

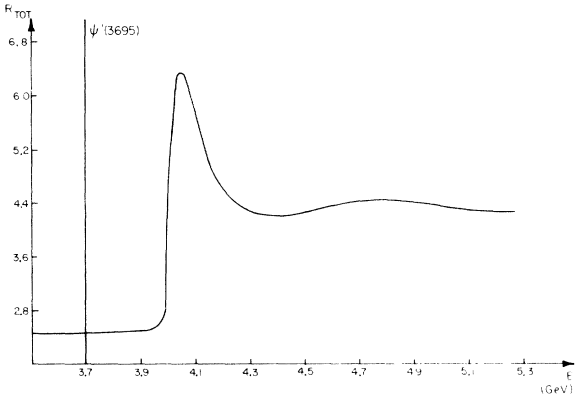

FIG. 9. R computed for the potential in Fig. 8.

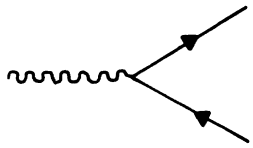

FIG. 10. A light-quark pair materializing from a gluon.

index j. Let ψ_{jl}^{ki} denote the wave function of a charmed meson–anticharmed meson pair. The meson (antimeson) is composed of a heavy quark with spin index i (j) and a light quark with spin index k (l). The two wave functions ψ_j^i and ψ_{jl}^{ki} define the two channels of a coupled-channel quantum-mechanics problem. The first channel consists of a $\mathcal{C}'\bar{\mathcal{C}}'$ pair. The potential which acts in this channel is just the unscreened potential $G(r)$. Later we shall assume that it is a linearly rising potential with an additional but small Coulomb attraction as in Eq. (1.1). Note that $G(r)$ would bind two-body $\mathcal{C}'\bar{\mathcal{C}}'$ states of arbitrarily large mass. The second channel consists of various species of charmed-anticharm meson pairs. The potential which acts in this channel, $Y(r)$, presumably has a typical short range characteristic of ordinary hadronic physics. In principle, it should depend on the spins of the constituents making up the mesons. It will not play a very important role in what follows so we shall let it be a short-range Yukawa repulsive potential.

The final ingredient in the model is the potential which mixes the two channels. We shall rely on our experience with quark-confining theories and use some elementary facts about hadronic forces in constructing a plausible coupling potential. First, recall that it should represent the creation of a light-quark pair. The form of the coupling will be taken from the low-energy behavior of graph in Fig. 10, where a vector gluon generates a light-quark pair in a spin-triplet, relative S wave. The spins of the heavy quarks are undisturbed by this process. These features suggest the interaction energy coupling the two channels,

$$H_{\text{int}} = \frac{1}{\sqrt{2}} \int d\vec{\mathbf{r}}\, \psi_i^{*j}(r) f(r) \hat{r} \cdot \vec{\tau}_k^l \psi_{jl}^{ki}(r), \tag{5.1}$$

where $f(r)$ is a scalar function of r, the distance between the heavy quarks, and $\vec{\tau}$ is a Pauli spin vector. The quantity $(1/\sqrt{2})(\hat{r}\cdot\vec{\tau})_k^l$ insures that the light quarks are produced in an S-wave spin triplet. Models of $f(r)$ will be discussed below. If we add H_{int} to the free Hamiltonians controlling the two uncoupled channels, we obtain the following two coupled Schrödinger equations,

$$\begin{aligned} -\frac{1}{2\mu_{\mathcal{C}'}} \nabla^2 \psi_j^i + G\psi_j^i + \frac{1}{\sqrt{2}} f(r) \hat{r}\cdot\vec{\tau}_k^l \psi_{jl}^{ki} &= E\psi_j^i, \\ -\frac{1}{2\mu_D} \nabla^2 \psi_{jl}^{ki} + Y\psi_{jl}^{ki} + \frac{1}{\sqrt{2}} f(r) \hat{r}\cdot\vec{\tau}_l^k \psi_j^i &= E\psi_{jl}^{ki}, \end{aligned} \tag{5.2}$$

where E is the c.m. energy of the system and $\mu_{\mathcal{C}'}$ (μ_D) is the reduced mass of two heavy quarks (charmed mesons). Now we should do some kinematic analysis to simplify the spin structure of these equations. We shall be mostly concerned with the $\psi(3.1)$ and $\psi'(3.7)$ in which the heavy quarks reside in an S-wave spin triplet. Therefore, consider

$$\psi_j^i = \frac{1}{\sqrt{2}} \hat{\epsilon}\cdot\vec{\tau}_j^i \psi(r), \tag{5.3}$$

where $\psi(r)$ is a scalar wave function and $\hat{\epsilon}$ is the polarization vector of the $\psi(3.1)$. The same observation motivates the ansatz,

$$\begin{aligned} \psi_{jl}^{ki} &= \frac{1}{\sqrt{2}} \hat{\epsilon}\cdot\vec{\tau}_j^i \bar{\psi}_l^k(r) \\ &= \tfrac{1}{2}(\hat{\epsilon}\cdot\vec{\tau})_j^i (\hat{r}\cdot\vec{\tau})_l^k \phi(r). \end{aligned} \tag{5.4}$$

Substituting Eqs. (5.3) and (5.4) into the Schrödinger equations gives

$$\frac{1}{2\mu_{\mathcal{C}'}} p_r^2 \psi + G\psi + f\phi = E\psi, \tag{5.5a}$$

$$\frac{1}{2\mu_D}\left(p_r^2 + \frac{2}{r^2}\right)\phi + Y\phi + f\psi = E\phi, \tag{5.5b}$$

where p_r is the radial momentum, $-i(1/r)(\partial/\partial r)r$, and the centrifugal barrier term has appeared in Eq. (5.5b) in the usual way. It reflects the fact that the outgoing charmed hadrons are produced in a p wave.

Now we generate coupled radial wave equations in a conventional form by defining radial wave functions,

$$\psi = u'/r, \quad \phi = \omega'/r. \tag{5.6}$$

Then Eqs. (5.5) become

$$\left[\begin{pmatrix} -\frac{1}{2\mu_{\mathcal{C}'}}\frac{d^2}{dr^2} & 0 \\ 0 & -\frac{1}{2\mu_D}\frac{d^2}{dr^2} \end{pmatrix} + \begin{pmatrix} G(r) & f(r) \\ f(r) & Y(r) + \frac{2}{2\mu_D r^2} \end{pmatrix}\right] \begin{pmatrix} u' \\ \omega' \end{pmatrix} = E \begin{pmatrix} u' \\ \omega' \end{pmatrix}. \tag{5.7}$$

Given the functions G, Y, f and sufficient strength, this coupled set of equations can be solved for all energies E. Instead of proceeding with brute force, we will develop an approximation procedure which relies on two approximations:

(1) The $\mathcal{P}'$ quark is much heavier than the ordinary $\mathcal{P}$ and $\mathfrak{N}$ quarks.

(2) The forces which act between hadrons transfer only small momenta.

Introduce a 2×2 unitary transformation $U(r)$ which diagonalizes the potential energy matrix in Eq. (5.7); i.e., $U(r)$ has the property

$$U(r)\underline{V}(r)U(r)^{-1} = V_D(r)\,, \tag{5.8}$$

where

$$\underline{V}(r) = \begin{pmatrix} G(r) & f(r) \\ f(r) & Y(r) + \dfrac{2}{2\mu_D r^2} \end{pmatrix} \tag{5.9}$$

and $V_D(r)$ is diagonalized. Thus $U(r)$ is a *spatially dependent* rotation matrix which acts on the two-component wave function,

$$\Psi'(r) = \begin{pmatrix} u'(r) \\ \omega'(r) \end{pmatrix} \rightarrow \Psi(r) = U(r)\Psi'(r)\,. \tag{5.10}$$

Although $U(r)$ diagonalizes the potential-energy part of the coupled-channel problem it does not commute with the kinetic-energy operator. However, on the basis of statements (1) and (2) above it may be sensible to treat the commutators of U with the kinetic-energy operator as corrections to a zeroth-order completely diagonalized problem. To carry this scheme out, write $U(r)$ in the form

$$U(r) = \exp\left[-\frac{i}{2}\sigma_y\theta(r)\right]\,, \tag{5.11}$$

where $\theta(r)$ is a spatially dependent angle. Because of statement (2) above, we expect $\theta'(r)$ and $\theta''(r)$ to be small quantities in GeV units. Write Eq. (5.7) in the matrix form

$$[\underline{T} + \underline{V}(r)]\Psi' = E\Psi'\,, \tag{5.12}$$

where

$$\underline{T} = \begin{pmatrix} -\dfrac{1}{2\mu_{\mathcal{P}'}}\dfrac{d^2}{dr^2} & 0 \\ 0 & -\dfrac{1}{2\mu_D}\dfrac{d^2}{dr^2} \end{pmatrix}. \tag{5.13}$$

Substituting Eq. (5.10) and multiplying through by $U(r)$ allows the differential equation to be written as

$$[U(r)\underline{T}U(r)^{-1} + V_D(r)]\Psi = E\Psi\,. \tag{5.14}$$

It is straightforward to compute

$$U(r)\underline{T}U(r)^{-1} = \underline{T} + \underline{C}(r)\,, \tag{5.15}$$

where

$$\underline{C}(r) = -\frac{1}{2\mu_{\mathcal{P}'}}\left[i\sigma_y\left(\theta'\frac{d}{dr} + \tfrac{1}{2}\theta''\right)\right] + \frac{1}{8\mu_{\mathcal{P}'}}(\theta')^2 - \left(\frac{\mu_{\mathcal{P}'} - \mu_D}{4\mu_{\mathcal{P}'}\mu_D}\right)[(\cos\theta - 1)\sigma_z + \sin\theta\sigma_x]\frac{d^2}{dr^2} + O\left(\frac{\mu_{\mathcal{P}'} - \mu_D}{2\mu_{\mathcal{P}'}\mu_D}\theta'\right)\,. \tag{5.16}$$

The last term in the expression for $\underline{C}(r)$ denotes several terms which are at least second order in the quantities $\mu_{\mathcal{P}'} - \mu_D/\mu_D\mu_{\mathcal{P}'}$ and θ', each of which are presumed to be small. One could, of course, study them in detail, but for the models to be analyzed below they prove to be negligible. Note that the second term in $\underline{C}(r)$ is also second order and can be dropped. The most interesting term in $C(r)$ will in fact prove to be the first one,

$$-\frac{1}{2\mu_{\mathcal{P}'}}i\sigma_y\left(\theta'\frac{d}{dr} + \tfrac{1}{2}\theta''\right)\,. \tag{5.17}$$

Anyway, in complete generality, Eq. (5.14) now has the form

$$(\underline{T} + V_D + \underline{C})\Psi = E\Psi\,. \tag{5.18}$$

Suppose that the matrix elements of $\underline{C}(r)$ are small compared to the other terms in this equation. Then it would be sensible to solve Eq. (5.18) iteratively. We write

$$\Psi = \Psi^{(0)} + \Psi^{(1)} + \cdots \tag{5.19}$$

and substitute back into the differential equation

$$(\underline{T} + V_D)\Psi^{(0)} = E\Psi^{(0)}\,, \tag{5.20a}$$

$$(\underline{T} + V_D - E)\Psi^{(1)} = -\underline{C}\Psi^{(0)}, \quad \text{etc.} \tag{5.20b}$$

where $\Psi^{(i)}$, $i > 0$, are the inhomogeneous solutions to this system of equations.

Now let us identify the zeroth-order Eq. (5.20a). Define

$$V_D(r) = \begin{pmatrix} \lambda_-(r) & 0 \\ 0 & \lambda_+(r) \end{pmatrix} = U(r)\underline{V}(r)U(r)^{-1}\,. \tag{5.21}$$

The eigenvalues $\lambda_\pm(r)$ are

$$\lambda_\pm(r) = \frac{1}{2}\left[G(r) + Y(r) + \frac{2}{2\mu_D r^2}\right] \pm \frac{1}{2}\left\{\left[G(r) - Y(r) - \frac{2}{2\mu_D r^2}\right]^2 + 4f^2(r)\right\}^{1/2}\,. \tag{5.22}$$

The potentials $G(r)$ and $Y(r)+2/2\mu_D r^2$ are shown schematically in Fig. 11. We expect that $f(r)$ has the form also shown in Fig. 11. Why is this? Recall that $f(r)$ is proportional to the probability that a light-quark pair materialize in the gluon field between a heavy $\mathcal{P}'\bar{\mathcal{P}}'$ pair. For small heavy-quark separation where the gluon field is necessarily small, $f(r)$ should be small, as depicted in the figure. However, as r grows, it should become probable for a light-quark pair to materialize. Therefore, let $f(r)$ be appreciable for r in the neighborhood of m_π^{-1} which is the characteristic length where strong interactions appear to be quite strong. Accepting the qualitative features of Fig. 11 we can now understand the qualitative features of the eigenvalues $\lambda_\pm(r)$, and the associated eigenfunctions $\Psi_\pm^{(0)\prime}$. At small r, f is negligible so

$$\lambda_+(r)\simeq Y(r)+\frac{2}{2\mu_D r^2}, \quad \Psi_+^{(0)\prime}\simeq\begin{pmatrix}0\\1\end{pmatrix}$$

and

$$\lambda_-(r)\simeq G(r), \quad \Psi_-^{(0)\prime}\simeq\begin{pmatrix}1\\0\end{pmatrix}.$$

This means that at short distances $\Psi_-^{(0)\prime}$ is purely in the $\mathcal{P}'\bar{\mathcal{P}}'$ sector. So the reaction $\gamma^*\to$ hadrons is sensitive to *only* $\lambda_-(r)$ and $\psi_-^{(0)\prime}(r)$ in the zeroth-order approximation to Eq. (5.20). Now, as r increases, $f(r)$ becomes appreciable and allows the potentials in Fig. 11 to mix. The smaller eigenvalue $\lambda_-(r)$ therefore approaches the smaller potential $Y(r)+2/2\mu_D{}^2r^2$ as $r\to\infty$ and $\lambda_+(r)\to G(r)$ as $r\to\infty$. It follows that $\Psi_+^{(0)\prime}\to\binom{1}{0}$ and $\Psi_-^{(0)\prime}\to\binom{0}{1}$ as $r\to\infty$. Thus $\Psi_-^{(0)\prime}$ falls purely in the charmed-hadron sector at large distances. This means that

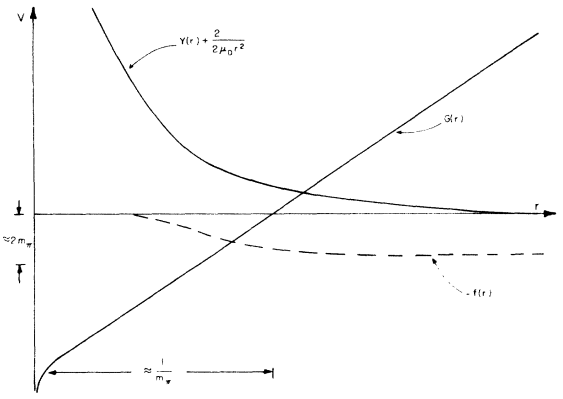

FIG. 11. Plausible shapes and magnitudes of the potentials $G(r)$, $Y(r)$, and $f(r)$. Note the estimate of the scales written in terms of m_π on the axes.

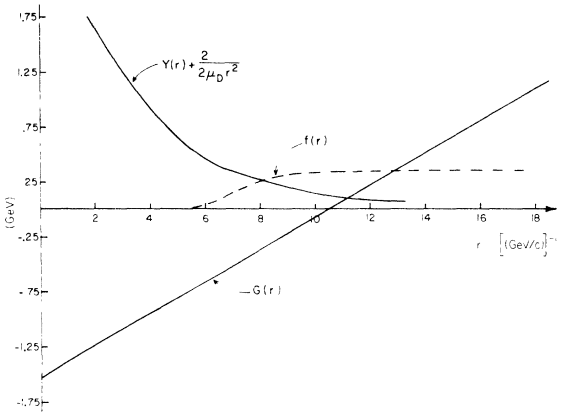

FIG. 12. Specific choice of the potentials $G(r)$, $Y(r)$, and $f(r)$ used in several model calculations.

the lowest-energy state of the system is purely heavy-quark—like at short distances and experiences the linear unscreened potential, but at large distances it becomes pure charmed-hadron–like and experiences typical hadronic forces. Thus, the picture which results is the adiabatic approximation discussed more intuitively in the previous section.

It is instructive to work out examples of $V_D(r)$ and $\Psi_\pm^{(0)}(r)$. Choose, as shown in Fig. 12,

$$\begin{aligned} G(r)&=0.16r-1.6,\\ Y(r)&=3.13e^{-0.20r},\\ f(r)&=0.16[1+\tanh(1.3r-9.1)], \end{aligned} \tag{5.23}$$

where all quantities which are not dimensionless

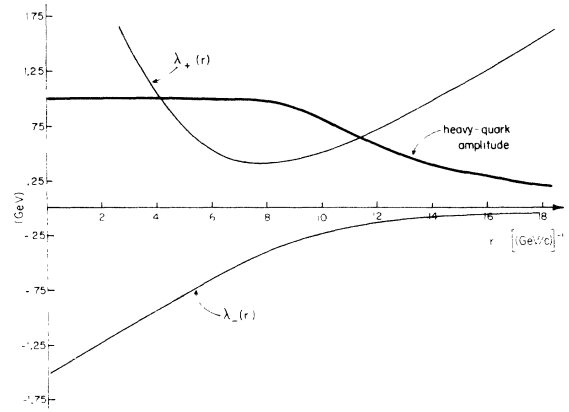

FIG. 13. The potentials $\lambda_-(r)$, $\lambda_+(r)$ and the heavy-quark amplitude,

$$(1,0)U(r)\begin{pmatrix}1\\0\end{pmatrix},$$

computed for the choices in Fig. 12.

are in GeV units. Note that the range of $Y(r)$ is on the order of m_π^{-1} and $f(r)$ is at most 320 MeV which is $O(m_{\mathcal{P}'})$ and/or the momentum fluctuations in hadronic matter. Then the potentials $\lambda_-(r)$, $\lambda_+(r)$ and the heavy-quark amplitude in the physical state, $\langle \mathcal{P}'|\Psi_-^{(0)\prime}(r)\rangle$, are shown in Fig. 13. We note that $\lambda_-(r)$ has roughly the same features as the screened quark potentials arrived at from different arguments in previous sections. Note also that $\langle \mathcal{P}'|\Psi_-^{(0)\prime}(r)\rangle$ changes smoothly from unity to zero over the spatial region where $f(r)$ is changing. In other words, the state vector converts smoothly from a pair of heavy quarks at small distances to an outgoing pair of charmed hadrons. The similarity of this now well-formulated statement to the adiabatic picture of the ionization of a hydrogen molecule into two free hydrogen atoms is interesting.

It should be clear that the zeroth-order approximation to Eqs. (5.20) reproduces the model results concerning R found in the previous section. By adjusting the various parameters at our disposal one obtains a $\lambda_-(r)$ potential which binds an S-wave ground state and its first excited state. Then the $3S$ state lies above the threshold and gives the $\psi''(4.1)$ enhancement studied earlier. Before turning to more calculations let us anticipate some of the new effects brought about by the coupled-channel model. The model begins with the potential $G(r)$ which is screened by $f(r)$ into the potential $\lambda_-(r)$. If we choose $G(r)$ to have the form of that used by Eichten *et al.*,[7] then $\lambda_-(r)$ will always have non-negligible curvature near its ionization point. Therefore, the $\psi'(3.7)$ wave function will occupy a larger volume than previously estimated. We expect that the ratio of the leptonic widths of the $\psi(3.1)$ and the $\psi'(3.7)$, and the $2S-2P$ mass difference will be sensitive to this effect. Calculations of these quantities will be done in a later section following an analysis of the first-order corrections to the adiabatic approximation.

A few words about the curious $\lambda_+(r)$ potential are in order. At the level of the zeroth-order approximation the potential $\lambda_+(r)$ and its eigenfunction $\Psi_+^{(0)\prime}$ can be ignored. However, we shall see that $\lambda_+(r)$ indirectly produces some interesting corrections to the lowest-order adiabatic picture. We note that for small r, $\lambda_+(r)$ is well approximated by $Y(r)+2/2\mu_D r^2$, so $\lambda_+(r)\to\infty$ as $r\to 0$. Similarly, for larger r $\lambda_+(r)$ becomes $G(r)$, so $\lambda_+(r)\to\infty$. These features will obviously be true of a wide class of models and they may be important since they guarantee that the spectrum of $\lambda_+(r)$ is *discrete*. In potential models the discrete spectrum of $\lambda_+(r)$ also exists to infinity, but recall that the entire approach envisioned here is only trustworthy near the threshold. It is very questionable whether the high-energy behavior of $\lambda_+(r)$ is compatible with local quantum field theory, but it is reasonable to trust $\lambda_+(r)$ in the vicinity of its lowest few bound states. Comparing Figs. 11 and 13 we see that the spectrum of $\lambda_+(r)$ will closely approximate the spectrum of $G(r)$ above its $3S$ level. But the centrifugal barrier in $\lambda_+(r)$ insures that these states do not have appreciable values at the origin and do *not* directly contribute to R. Their role is more subtle and will be studied in the next section.

VI. CORRECTIONS TO THE ADIABATIC APPROXIMATION

Now return to Eq. (5.20) and consider the first correction, $\Psi^{(1)}$, to the adiabatic state vector $\Psi^{(0)}$,

$$(\underline{T}+V_D-E)\Psi^{(1)}=-\underline{C}\Psi^{(0)}. \tag{6.1}$$

There are two classes of terms in $\underline{C}$ of a rather different character, so we shall consider them separately. First, there are terms which are diagonal, such as

$$-\left(\frac{\mu_{\mathcal{P}'}-\mu_D}{4\mu_{\mathcal{P}'}\mu_D}\right)[(\cos\theta-1)\sigma_z]\frac{d^2}{dr^2}. \tag{6.2}$$

Let us estimate this term's effect on the eigenvalues of the zeroth-order approximation. Replace d^2/dr^2 by $-p^2$, and let $\frac{1}{2}(\cos\theta-1)$ have its maximum value of -1. Then, keeping this correction we have the replacement

$$\begin{pmatrix}\lambda_- & 0\\ 0 & \lambda_+\end{pmatrix}\to\begin{pmatrix}\lambda_- - \dfrac{\Delta\mu}{2\mu_{\mathcal{P}'}\mu_D}p^2 & 0\\ 0 & \lambda_+ + \dfrac{\Delta\mu}{2\mu_{\mathcal{P}'}\mu_D}p^2\end{pmatrix}, \tag{6.3}$$

where $\Delta\mu=\mu_{\mathcal{P}'}-\mu_D$. Therefore, the zeroth-order approximation will be good only if

$$\frac{\Delta\mu}{2\mu_{\mathcal{P}'}\mu_D}p^2\ll 1. \tag{6.4}$$

We expect $\Delta\mu\approx 300$ MeV, $\mu_D\approx 2$ GeV, so this requirement reads

$$p^2/2\mu_D\ll 7. \tag{6.5}$$

Thus, we can neglect this correction to the zeroth-order approximation as long as we consider only energies within 2 GeV, say, of threshold.

In fact, when the system of equations was analyzed numerically, *diagonal* terms such as Eq. (6.2) were simply incorporated into the zeroth-order equation. Therefore, we were not limited directly by the inequality above. However, since we are using a nonrelativistic formalism we can-

not believe the calculations except within several GeV of threshold anyway.

The second class of terms in $\underline{C}$ which generate more interesting corrections involve *off-diagonal* Pauli matrices. We shall illustrate the physics of such terms by concentrating on the first term in Eq. (5.16).

$$\underline{C}(r) = -\frac{1}{2\mu_D}\left[i\sigma_y\left(\theta'\frac{d}{dr} + \tfrac{1}{2}\theta''\right)\right] + \cdots . \tag{6.6}$$

It is convenient to write

$$\Psi^{(0)} = \begin{pmatrix} u_0 \\ \omega_0 \end{pmatrix}, \quad \Psi^{(1)} = \begin{pmatrix} u_1 \\ \omega_1 \end{pmatrix} \tag{6.7}$$

and to write out the differential equation for u_1,

$$\left[-\frac{1}{2\mu_{\mathcal{O}'}}\frac{d^2}{dr^2} + \lambda_-(r) - E\right]u_1(r) = \frac{1}{2\mu_D}\left(\theta'\frac{d}{dr} + \tfrac{1}{2}\theta''\right) \times \omega_0(r) , \tag{6.8}$$

where ω_0 satisfies the equation

$$\left[-\frac{1}{2\mu_D}\frac{d^2}{dr^2} + \lambda_+(r) - E\right]\omega_0(r) = 0 . \tag{6.9}$$

Therefore, the functions $\omega_0(r)$ are the eigenstates of the discrete spectrum of $\lambda_+(r)$. This means that the source term in Eq. (6.8) is nonzero only for energies near the bound states of $\lambda_+(r)$ and that there are *no* first-order corrections to $u_0(r)$ except near these energies. If the overlap of $-C(r)\Psi^{(0)}$ with $\Psi^{(0)}$ itself is sufficiently small, then the corrections to the zeroth-order calculation of R will be small (i.e., involve little change in the *area* under the curve R versus E) and will be well isolated around the energies of the bound states of $\lambda_+(r)$.

To analyze the coupled differential equations in a quantitative, systematic fashion, view them as a coupled-channel problem of the following sort.[33] Define the first channel as the Schrödinger equation with the potential $\lambda_-(r)$. Label its spectrum of states $\{u_i^{(0)}\}$ and its energy eigenvalues $\{\epsilon_i^-\}$. The $\{u_i^{(0)}\}$ contains several discrete states, the $\psi(3.1), \psi(3.7)$, various $l=1$ levels, etc., and a continuum above the ionization point of $\lambda_-(r)$. Define the second channel as the Schrödinger equation in the potential $\lambda_+(r)$. The spectrum of this problem consists of only discrete levels $\{\omega_i^{(0)}\}$ and discrete energies $\{\epsilon_+^i\}$. Finally these channels are coupled through the interaction

$$\underline{C}(r) = -\frac{1}{2\mu_{\mathcal{O}'}}\left(\tfrac{1}{2}\theta'' + \theta'\frac{d}{dr}\right)i\sigma_y + \cdots . \tag{6.6'}$$

These ingredients can now be fed into a coupled-channel formalism.[34] Only the results of that exercise will be stated here. They can be reproduced upon consulting Ref. 34. First, each level $\{\omega_i^{(0)}\}$ in the potential $\lambda_+(r)$ obtains a width through its coupling to continuum states:

$$\Gamma_i(E) = 2\pi\left|\langle \omega_i^{(0)} | \underline{C} | u_E^{(0)}\rangle\right|^2 , \tag{6.10}$$

where $u_E^{(0)}$, the eigenstate of the $\lambda_-(r)$, satisfies outgoing boundary conditions. The shift of each level is obtained through the dispersive integral,

$$\Delta_i(E) = \frac{1}{2\pi}\mathrm{P}\int\frac{\Gamma_i(E')dE'}{E - E'} . \tag{6.11}$$

And finally, the corrected wave function (outgoing boundary conditions) is

$$u_E(r) \cong u_E^{(0)} + u_E^{(1)} + \cdots , \tag{6.12a}$$

where, for E near ϵ_i^+,

$$u_E^{(1)}(r) \cong \left[\frac{\underline{C}(r)\omega_i^{(0)}(r)}{E - \epsilon_i^+ + \frac{1}{2}i\Gamma_i(E) - \Delta_i(E)}\right] \times \int G_-(E; r'r)\underline{C}(r')\omega_i^{(0)}(r')u_E^{(0)}(r')dr' . \tag{6.12b}$$

The quantity $G_-(E; r', r)$ in Eq. (6.12b) is the outgoing Green's function calculated in the single-channel $\lambda_-(r)$ potential. The validity of Eq. (6.12) is limited by the assumption that the states $\omega_i^{(0)}(r)$ do not overlap. This assumption will be verified explicitly for the models of $\underline{C}(r)$ discussed in the previous section.

Now let us summarize our analyses of Eqs. (6.10)–(6.12) in a class of models which include the choice of potentials sketched in Figs. 11–13. There are several tasks one must perform,

(1) determine the spectrum $\{\omega_i, \epsilon_i^+\}$,

(2) compute the widths $\Gamma_i(E)$ and shifts $\Delta_i(E)$ of these states, and

(3) determine the Green's function $G_-(E; r', r)$ for the potential $\lambda_-(r)$,[35]

before one can evaluate $u_E^{(1)}(r)$ from Eq. (6.12). Finally, after properly normalizing the continuum state $u_E(r) = u_E^{(0)}(r) + u_E^{(1)}(r)$ to unit flux at infinity, one evaluates $u_E(0)$ and determines a new R from Eq. (4.5). Most of this work must be done numerically, but the trends of the results can be understood simply. First, the low-lying spectrum of $\lambda_+(r)$ must be determined. For the potentials of Fig. 12 one finds

$$\begin{aligned} \epsilon_1^{(+)} &\cong 4.55 \text{ GeV} , \\ \epsilon_2^{(+)} &\cong 4.86 \text{ GeV} \end{aligned} \tag{6.13}$$

and the states $\omega_1^{(0)}(r)$ and $\omega_2^{(0)}(r)$ are shown in Fig. 14. Note that the lowest state $\omega_1^{(0)}(r)$ is well approximated by a smooth Gaussian which *vanishes* near the origin because of the presence of

the centrifugal barrier in $\lambda_+(r)$. It is trivial now to compute the widths $\Gamma_i(E)$:

$$\Gamma_1 \approx 1.5 \text{ MeV}, \quad \Gamma_2 \approx 16 \text{ keV}. \tag{6.14}$$

These widths are very small on the scale of $E_{\text{c.m.}} \approx 4.5$ GeV. There are two reasons for this:

(1) The goodness of the adiabatic approximation is one reason—the functions $\lambda_\pm$ and f are smooth so θ' and θ'' are small in GeV units.

(2) The overlap integrals in Eq. (6.10) involve ω_i which extend over a large segment of the r axis. After applying $\underline{C}(r)$, they are then folded against $u_E^{(0)}(r)$ which is a continuum state several hundred MeV above threshold. Thus, $u_E^{(0)}(r)$ oscillates several times within the important integration region and the overlap integral can be an order of magnitude smaller than an uneducated guess.

The analysis also shows that the value $\Gamma_2 \approx 16$ keV is somewhat misleading since $\Gamma_2(E)$ is a rapidly varying function of E in the neighborhood of $\epsilon_2^{(+)}$.

The results of Eq. (6.14) were considered somewhat peculiar so the calculation was repeated for various other choices of potentials. A second set of potentials is shown in Fig. 15. In this case a smoother $f(r)$ was chosen,

$$f(r) = 0.39[1 + \tanh(0.25r - 1.75)], \tag{6.15}$$

with rather similar curves for $\lambda_\pm(r)$ resulting. Therefore, the simpler consequences of Fig. 15 will be very similar to those of Fig. 13. However, as indicated above, Γ_i involve some subtle effects. In this case one computes

$$\Gamma_1 = 4 \text{ keV}, \quad \Gamma_2 = 6 \text{ MeV}. \tag{6.16}$$

Again, Γ_1 and Γ_2 are very small but the roles of 1 and 2 have (in a rough sense) been interchanged. As before, the precise value for Γ_1 is deceptive since it changes rapidly with E. A more meaningful measure of the effect of the states $\omega_i^{(0)}(r)$ on the continuum is obtained by calculating R.

Before tabulating the results of a calculation of R, consider the character of Eq. (6.12). Note that the relative phases of $u_E^{(1)}(r)$ relative to $u_E^{(0)}(r)$ relative to $u_E^{(0)}(r)$ determine whether $|u_E(0)|^2$ will be larger or smaller than $|u_E^{(0)}(0)|^2$. But the value of such phases [which determine whether there is constructive or destructive interference between $u_E^{(1)}(0)$ and $u_E^{(0)}(0)$] depends on subtle overlap integrals and the precise value of E chosen. It will be apparent in the results that the relative phases of $u_E^{(0)}$ and $u_E^{(1)}$ can be very different at $\epsilon_1^{(+)}$ and $\epsilon_2^{(+)}$.

For the potentials of Fig. 13 we found that the effect on R near $\epsilon_1^{(+)}$ was negligible (a slight depression) while a narrow "glitch" appeared in R near $\epsilon_2^{(+)}$, as shown in Fig. 16. For the potentials of Fig. 15, a similar glitch appears in R near $\epsilon_1^{(+)}$ while only a negligible and wider depression appeared near $\epsilon_2^{(+)}$. Note the narrow width, 30 keV, and the occurrence of both destructive and constructive interference in Fig. 16.

Since these glitches are very narrow and not

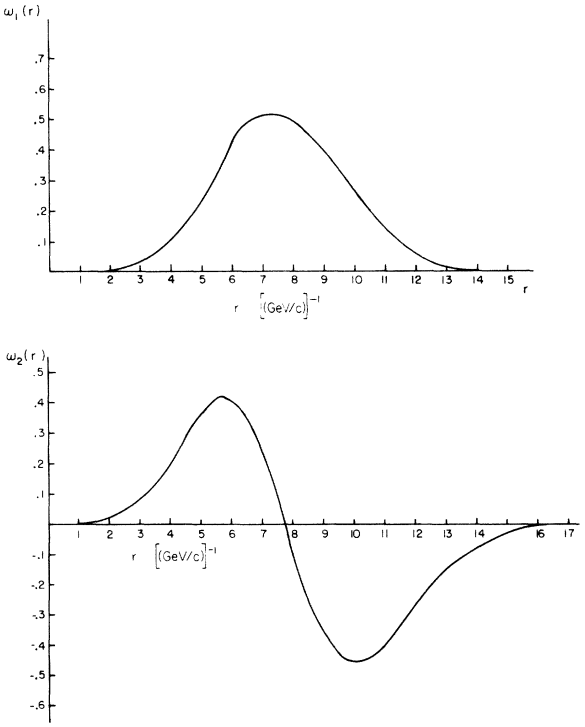

FIG. 14. (a) Ground state of $\lambda_+(r)$ potential shown in Fig. 13. (b) First excited state of $\lambda_+(r)$.

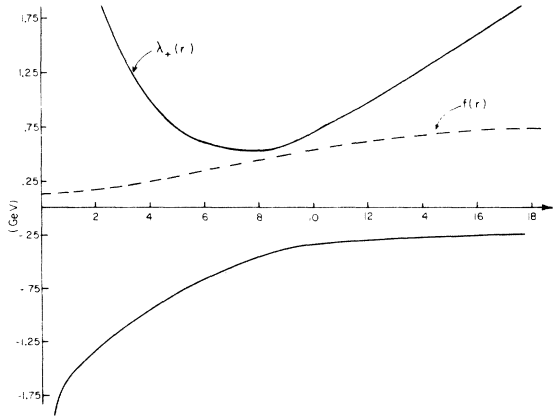

FIG. 15. The potentials λ_-, λ_+ and f corresponding to Eq. (6.15) for f, $G(r) = -(0.177/r)(1-r^2) - 1.56$ and $Y(r) = 0.313e^{-0.32r}$.

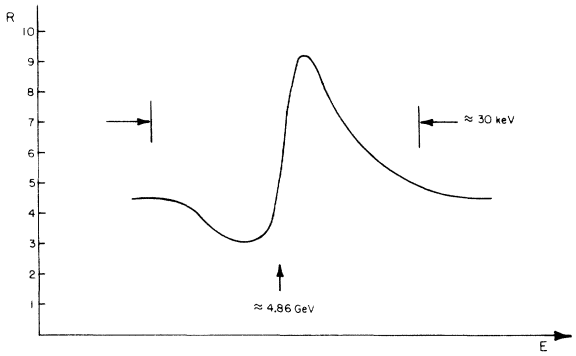

FIG. 16. The glitch near $\epsilon_2^{(+)}$ calculated for the potentials in Fig. 12. Note the expanded energy scale. The glitch is only ≈ 30 keV wide.

high enough to subtend much area they will be very difficult to observe experimentally. These two examples emphasize that the existence of glitches depends on phases in Eq. (6.12) which are sensitive to the details of each model. However, experience has suggested that if a glitch does not occur at $\epsilon_i^{(+)}$ then a glitch will appear near $\epsilon_{i+1}^{(+)}$. It appears that the energy dependence of the relative phases is responsible for this regularity. Therefore, perhaps it is not too unreasonable to expect a glitch at one of the two energies $\epsilon_1^{(+)}, \epsilon_2^{(+)}$.

These effects are rather odd, but similar phenomena do appear in systems containing nuclear and/or atomic resonances. In fact, the sensitivity of the shape of glitches to the phase of the continuum has been noted in these contexts.[34] However, the glitches we are discussing are very *small* effects (they are narrow and subtend small area) so we wonder whether they survive in more realistic models. For example, models with multibody final states contain more amplitudes which could interfere with these glitches and wash them out. At a more basic level, it is not clear that the coupled-channel model embodies the screening mechanism of field theories which prohibit asymptotic states of quarks with enough accuracy to be trusted in their minute details. We find this last remark particularly worrisome. Nonetheless, it seems worthwhile to point out these curious phenomena since they are a reflection of quark confinement in these simple models. If glitches were ever to be discovered in R, they could be interpreted as evidence for the existence of long-range forces in the theory underlying conventional hadronic physics.

VII. CORRECTIONS TO THE SIMPLE QUARK PICTURES OF CHARMONIUM

Quark models of charmonium[7,8,13] phenomenology were developed immediately after the discovery of the ψ and the ψ'. These models ignored the influence of the nearby threshold on the spectrum of heavy-quark bound states. In this section we wish to estimate some of the corrections to these models coming from a coupled-channel analysis.

First, note that the $\psi(3.1)$ and the $\psi'(3.7)$ are *no longer* simple two-quark bound states. This fact is apparent in the zeroth-order adiabatic approximation. Recall that to diagonalize the potential $V(r)$ in Eq. (5.12) a similarity transformation $U(r)$ was introduced with the properties

$$U(r)V(r)U(r)^{-1} = V_D(r)\,, \quad \Psi(r) = U(r)\Psi'(r)\,.$$

Recall from Eq. (5.7) that the upper component of Ψ' is in the pure heavy-quark sector while its lower component is in the pure charmed-meson sector,

$$\Psi'(r) = \begin{pmatrix} u'(r) \\ \omega'(r) \end{pmatrix}. \tag{5.10}$$

The 3.1 and 3.7 states are described by the states of the form

$$\Psi^{(0)}(r) = \begin{pmatrix} u^0(r) \\ 0 \end{pmatrix} \tag{5.19'}$$

in the lowest-order adiabatic approximation. The amplitude that this vector lies in the quark sector is

$$A_{\psi'}(r) = (1,0)U(r)^{-1}\begin{pmatrix} u^0(r) \\ 0 \end{pmatrix}$$

$$= (u^0(r), 0)\,U(r)\begin{pmatrix} 1 \\ 0 \end{pmatrix}, \tag{7.1}$$

while the amplitude that it lies in the charmed-hadron sector is

$$A_H(r) = (0,1)U(r)^{-1}\begin{pmatrix} u^0(r) \\ 0 \end{pmatrix}$$

$$= (u^0(r), 0)\,U(r)\begin{pmatrix} 0 \\ 1 \end{pmatrix}. \tag{7.2}$$

Let us discuss the qualitative features of these amplitudes. For small r, $U(r)$ is essentially the identity so $A_{\psi'}(r) \approx u^0(r)$ and $A_H(r) \approx 0$. However, as r increases, $U(r)$ effects the conversion of a system of heavy quarks into a system of heavy mesons. Thus

$$U(r) \to \begin{pmatrix} 0 & 1 \\ 1 & 0 \end{pmatrix}$$

as $r \to \infty$, which implies that $A_{\varphi'}(r) \to 0$ and $A_H(r) \to u^0(r)$ in this limit. In Fig. 13 we plotted a quantitative example which showed $(1,0)U(r)\binom{1}{0}$ in the transition region. Note that the transformation is nontrivial wherever $f'(r) \neq 0$ and that this is the same region where the $\lambda_-(r)$ is bending from a linearly rising to a constant potential. Since the $\psi'(3.7)$ lies near the threshold its wave function extends into this region and beyond. Therefore, the charmed-hadron piece of its wave function must be *considerable* for large r. The $\psi(3.1)$ is contained in a smaller volume so the amplitude that it is a bound state of two charmed hadrons is much smaller for the models constructed here.

Numerical studies of this effect show that its strength is sensitive to the shape of $f(r)$ and the nearness of the threshold. If one chose $f(r)$ to rise from zero at smaller r values than in Fig. 12, the charmed-hadron part of the $\psi(3.7)$ would be larger than in this example.

Another sizeable correction to naive two-quark models of charmonium states concerns the shape of the potential acting between the heavy quarks. Consider the quark sector of the coupled channel model discussed in Sec. V. We suppose that the confining potential $G(r)$ acts in that sector so there exists a rich spectrum of heavy-quark bound states. Between the $1\,^1S$ and its first radial excitation $2\,^3S$, there is a family of $^3P_{2,1,0}$ states. Just below the $1\,^3S$ ($2\,^3S$) is its spin singlet partner $1\,^1S$ ($2\,^1S$). The spectrum has been discussed in further detail elsewhere.[7,13] It was hoped that the existence of this family of states could be confirmed by the observation of γ-ray transitions between them.[36] Using the potential of Eq. (1.1), the center of gravity of the P states was estimated at 230 MeV below the $2\,^3S$ state. Then the rates for the decays of $2\,^3S$ state into the $2\,^3P$ states could be calculated in the dipole approximation. The total widths for these transitions was found to be 215 keV, a large quantity, which suggested that γ rays would be easily detected in the final states of $\psi'(3.7)$ production. The calculations were noted to be quite model-dependent since the widths depend on the *cube* of the energy difference of the $2P$ and the $2S$ states and on the *square* of the matrix element of the dipole operator between these states. We now repeat these calculations in the coupled-channel model. Now the potential $\lambda_-(r)$ binds the charmonium states so the energy spacings are changed. In fact, it is easy to see that the $2P$-$2S$ energy difference in the λ_- potential is necessarily *less* than the same energy difference in the $G(r)$ potential. The reason is that the $\lambda_-(r)$ potential has curvature near its ionization point—it bows outward, as in Figs. 13 and 15. Since the $2S$ state has a node and the $2P$ states do not, increasing the curvature of the potential generally *decreases* the $2S$-$2P$ energy *difference*. Examples of this trend are the following: In a harmonic potential the $1S$-$2P$-$2S$ states are equally spaced, in a linear potential the $2P-2S$ energy difference is less than the $1S-2P$ difference, and in the Coulomb potential the $2P$ and $2S$ states are degenerate.

The spectrum of states of λ_- potentials were obtained numerically. The calculations employed a potential $G(r)$ whose Coulomb term had a strength suggested by asymptotic freedom ($\alpha_s \approx 0.2$) and a linear term suggested by the string model (κr, $\kappa \approx (2\pi)^{-1}$). In addition, the heavy-quark mass was chosen in the range 1.6–1.8 GeV and the depth of the potential was adjusted so that the threshold appeared between 3.8 and 4.0 GeV. Using the coupling potentials $f(r)$ in Eq. (5.23) and (6.15) it was not difficult to obtain $\lambda_-(r)$ potentials which bind the $\psi(3.1)$ and $\psi'(3.7)$ at the proper energies. Using $\lambda_-(r)$ wave functions and energy differences for all the states of interest were obtained. The $2S-2P$ energy differences which resulted lay in the range

$$\Delta E(2S-2P) = 120\text{–}170 \text{ MeV}. \tag{7.3}$$

The reason for the large spread in ΔE reflects the fact that the theoretical calculation is simply not sufficiently constrained to generate a unique answer. The $2S-2P$ energy difference is sensitive to the curvature in λ_- near threshold. By varying the position of the threshold and the form of f a range of $\Delta E(2S-2P)$ results as in Eq. (7.3). For all these $\lambda_-(r)$ the $\psi(3.1)$ and $\psi'(3.7)$ have the correct energy difference. Note, as expected, that the new ΔE are considerably smaller than 230 MeV. The following trend in the calculations was also noted with interest: The nearer the threshold was placed to the $\psi'(3.7)$ the smaller ΔE became. Corresponding to Eq. (7.3), one computes the radiative widths

$$\begin{aligned} &\Gamma_\gamma(2\,^3S \to 2\,^3P_2) = 17\text{–}48 \text{ keV}, \\ &\Gamma_\gamma(2\,^3S \to 2\,^3P_1) = 10\text{–}28 \text{ keV}, \\ &\Gamma_\gamma(2\,^3S \to 2\,^3P_0) = 3.5\text{–}10 \text{ keV}, \end{aligned} \tag{7.4}$$

where we have left the matrix element unchanged from the naive calculation.[7] Thus, the total contribution to the width of the ψ' from decay into P states is

$$\Gamma_\gamma(2\,^3S_1 \to \sum_J 2\,^3P_J) = 20.5\text{–}86 \text{ keV}. \tag{7.5}$$

The total width of the ψ' is approximately 250 keV,[1] so the branching ratio into P states is

$$\frac{\Gamma_\gamma(2\,^3S_1 \to \sum_J 2\,^3P_J)}{\Gamma_{\text{tot}}(\psi')} = 8\text{–}34\%\,. \tag{7.6}$$

The present experimental upper bound on $\Gamma(\psi' \to \gamma + \text{anything})/\Gamma(\psi' \to \text{anything})$ is on the order of several percent. Therefore, accounting for this single effect, the reduction of the $2S-2P$ energy difference, reduces significantly the discrepancy with experiment.

Before discussing Eq. (7.6) critically, let us calculate the ratio of the leptonic decay widths of the $\psi(3.1)$ and the $\psi'(3.7)$. In bound-state models, it is natural to study the ratio[7]

$$\eta = \left|\frac{u(1\,^3S; r=0)}{u(2\,^3S; r=0)}\right|^2 = \left(\frac{3.1}{3.7}\right)^2 \frac{\Gamma_e(\psi)}{\Gamma_e(\psi')}, \tag{7.7}$$

which is measured to be 1.5–1.6.[1] The nearness of the experimental number to unity was a motivating factor for incorporating confinement into the heavy-quark potential. Many authors observed that $\eta \equiv 1$ for a linear potential while $\eta = 8$ for a Coulomb potential. Using the potential $G(r)$ in Eq. (1.1) one can calculate $\eta = 1.05$, which is significantly smaller than the experimental value. It is clear, however, that the coupled-channel dynamics will *increase* this ratio. Since $\lambda_-(r)$ has an ionization point and curvature below it, the $2S$ state will be spread out over a larger volume [as compared to the same calculation in the potential $G(r)$]. Therefore, its value at the origin will be decreased and η will be increased. Numerical calculations of this ratio for potentials $\lambda_-(r)$ referred to above predict

$$\eta = \left|\frac{u(1\,^3S; r=0)}{u(2\,^3S; r=0)}\right|^2 = 1.5\text{–}1.6\,, \tag{7.8}$$

which is in the experimental range.

Consider briefly the effect of the mixing phenomena discussed in the second paragraph of this section on the results Eqs. (7.6) and (7.8). Since Eq. (7.8) involves only the wave function at the origin and since $U(r=0)=1$, the calculation of η is unaffected by this complication. However, the calculations of the γ-ray transitions involve the matrix element of the dipole operator between stationary states and these *can* be affected. Since the $\psi'(3.7)$ lies nearer to threshold than the P states, its wave function should have a larger charmed-meson component in it. However, the dipole operator does not mix charmed-meson and charmed-quark sections, so the rates $\Gamma_\gamma(\psi' \to {}^3P_J)$ may be further reduced by this effect. This point may be quite important in practice because the data[2] suggests—unlike our simplified models—that the ψ' lies just above a weak threshold at 3.6 GeV (a model with this feature will be discussed briefly in the next section). In the SU(4) scheme one would like to identify the 3.6-GeV threshold with $D\bar{D}$ production. After the experimental study of final states is carried out and the decay products of the ψ' are identified, it may be worthwhile to incorporate these qualitative ideas into quantitative model calculations.

VIII. FINAL STATES OF $\sigma(e^+e^- \to \text{hadrons})$ ABOVE THE NEW THRESHOLD

We wish to discuss briefly the composition of the final states of $\sigma(e^+e^- \to \text{hadrons})$ in the coupled-channel model introduced in Sec. V. It was constructed with spin-independent forces so there must be a simple relation between the number of spin-triplet charmed mesons (D^*) and spin-singlet charmed mesons (D).[37] The initial spin state of the quarks is

$$\frac{1}{\sqrt{2}}(\hat{\epsilon}\cdot\vec{\tau})^i_j \frac{1}{\sqrt{2}}(\hat{r}\cdot\vec{\tau})^k_l\,. \tag{8.1}$$

This expression states that the heavy quarks (spin labels i, j) are produced in a spin-triplet state by the photon of polarization $\hat{\epsilon}$, and the light quarks (labels k, l) are produced in a spin-triplet state between the heavy quarks ($\hat{r}$ points between the $\mathcal{P}'$ and $\bar{\mathcal{P}}'$). This state contains both spin-1 and spin-0 pieces,

$$\tfrac{1}{2}(\hat{\epsilon}\cdot\vec{\tau})^i_j(\hat{r}\cdot\vec{\tau})^k_l = (\tau^i_l)^\alpha(\tau^k_j)^\beta c_{\alpha\beta} + \tfrac{1}{2}\delta^i_l\,\delta^k_j c\,, \tag{8.2}$$

where c is the amplitude (normalized) to find a spin-zero configuration in the tensor product. Set $i=l$, $k=j$, and sum over the remaining indices,

$$\tfrac{1}{2}\,\mathrm{tr}\vec{\tau}\cdot\hat{\epsilon}\,\vec{\tau}\cdot\hat{r} = \tfrac{1}{2}(2)(2)c\,. \tag{8.3}$$

Since $\mathrm{tr}\tau_\alpha\tau_\beta = 2\delta_{\alpha\beta}$,

$$c = \tfrac{1}{2}\hat{\epsilon}\cdot\hat{r}\,. \tag{8.4}$$

Squaring and averaging over the angle between $\hat{\epsilon}$ and $\hat{r}$ gives the probability to have a $D\bar{D}$ final state,

$$\langle c^2\rangle_\Omega = \frac{1}{4}\frac{\int\cos^2\theta\, d\cos\theta}{\int d\cos\theta} = \frac{1}{12}\,. \tag{8.5}$$

Thus, in this model where the D and D^* are degenerate, the final states building up the large enhancement in R at 4.1 GeV would be composed mostly of the D^*.

It is tempting to consider intuitively the effect of the D-D^* mass splitting on these considerations.

Most investigations into broken SU(4) mass formulas,[37] or models of charm dynamics,[27] suggest that the D-D^* mass splitting is on the order of 100 MeV. Bold estimates state

$$m(D) = 1.83 \text{ GeV}, \quad m(D^*) = 1.95 \text{ GeV}, \qquad (8.6)$$

so the $D\bar{D}$ threshold (3.66 GeV) occurs very close to the ψ' and $D^*\bar{D}^*$ threshold occurs at 3.90 GeV. These estimates and the expectation that D^*'s will outnumber D's by a wide margin in the final states, suggest that R should

(1) begin to rise smoothly at 3.66 GeV owing to a relatively weak $D\bar{D}$ threshold, and

(2) rise swiftly at 3.90 GeV where the many spin states of the $D^*\bar{D}^*$ system can contribute.

The data do in fact resemble these qualitative expectations. A more sophisticated coupled-channel model with weak spin-dependent forces might be productive.

Note that these model considerations ignore the possibility that $\lambda\bar{\lambda}$ pairs are created by the forces between heavy quarks. The justification for this is the conventional wisdom that such processes are much less likely than those involving $\mathcal{P}$ and $\mathfrak{N}$ quarks. The relatively weak $F\bar{F}$ and $\bar{F}^*F^*$ thresholds can be included in similar models if desired.

Finally, it is amusing to observe that the $D^* - D$ mass difference is less than m_π. Therefore $D^* \to D + \gamma$ is probably the most likely decay of the D^*. Thus, two relatively low-energy ($\approx$100 MeV) photons should accompany most of the events which build up the 4.1-GeV enhancement in R.

IX. CONCLUDING REMARKS AND SPECULATIONS

In summary, it appears that simple charmonium models explain several experimental facts in a natural way. These include (1) the energy difference of the ψ, ψ', and ψ'', (2) the behavior of R in the immediate neighborhood of 4.0 GeV (e.g., the width and area under the ψ''), and (3) the ratio of the leptonic widths of the ψ and ψ'. Other facts, such as the ratio of the leptonic to hadronic widths of the ψ, can be understood as consequences of asymptotic freedom[31] without involving a detailed dynamical picture. However, the original SU(4) model in which one assumes that the ψ' and ψ'' are radial excitations of the ψ suffers from several potentially deadly problems. They include (1) the lack of evidence for a family of $2P_J$ states lying between the ψ and ψ', (2) the absence of charmed mesons of mass $\approx$2.0 GeV with the expected properties, and (3) the high value of R in the vicinity of 6.0 GeV. We have noted in the text that the $2P_J$ family of states may be more difficult to observe experimentally than originally expected[7,36] because the nearness of the threshold at 3.7–4.0 GeV tends to lower the $2S - 2P_J$ energy difference and tends to complicate the wave-function description of the ψ'. Both of these effects inhibit γ-ray transitions as estimated in the text. It is conceivable that the SU(4) charmonium picture will survive this problem although the experimental situation is discouraging. On the basis of the models discussed here, one *does* expect to find some γ rays with energies $\approx$150 MeV, but the rates as estimated in Sec. VII are quite small. Granting this, one is left with the problem of understanding the total width ($\approx$250 keV) of the ψ'. Experiments indicate that decays which do not involve the ψ give at least two neutral final-state particles. No explanation of this fact has been proposed. Problem (2) is, of course, very serious, but the theoretical estimates concerning the decay modes of charmed mesons are subject to considerable uncertainty and controversy. Finally, problem (3) is also most serious. Asymptotic-freedom estimates of R in the conventional SU(4) scheme predict $R \approx 3.7$ at $E \approx 6.0$ GeV.[29] The correction above 3.33 is calculated in second-order (renormalization-group improved) perturbation theory and the value of the running coupling constant used in the calculation is inferred from either (1) the approximate validity of Bjorken scaling in deep-inelastic scaling, or (2) the asymptotic-freedom estimate of the validity of Zweig's rule.[38] Most theorists agree that $\alpha_S \approx 0.2$ at $Q^2 \approx 10$ GeV^2.[31] If this is accepted and if R can be calculated in perturbation theory, then $R \approx 3.7$ is inescapable. One might criticize the perturbative calculation of R but one is then obliged to explain why the asymptotic-freedom estimate of R below charm threshold *does* agree with the data (2.2 versus 2.5 experimental). The high value of R has led to several 5- and 6-quark models.[11]

Consider briefly a model which predicts a curve of R versus E which fits all the available data. Suppose (just for the sake of argument) that one believes that the original SU(4) model will survive its difficulties concerning ψ, ψ' phenomenology and charm searches. Then the simplest (cheapest) way to bring the theoretical R into agreement with the data is to suppose that a heavy lepton $L^\pm$ exists. A comparison of Fig. 5 or Fig. 7 with the data[2] shows that the theoretical estimates are low for $E \gtrsim 4.6$–5.0 GeV. If the contribution of a heavy lepton having mass between 2.3 and 2.4 GeV is added to Fig. 5 or Fig. 7, then Fig. 17 results. Theory and experiment agree except, perhaps, for the highest-energy point. This detailed agreement encourages us to suggest

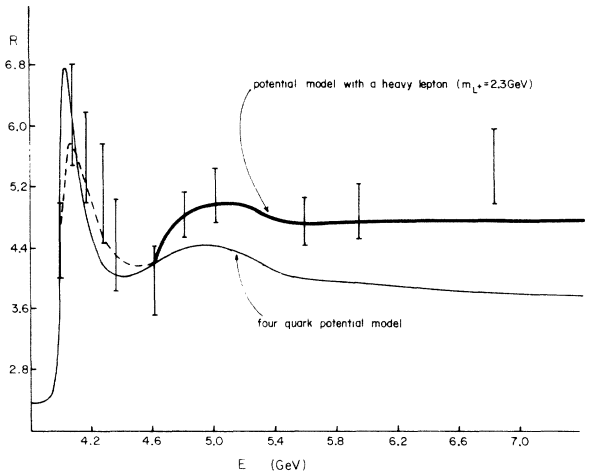

FIG. 17. Heavy-lepton ($m_{L^+}=2.3$ GeV) and four-quark contributions to R. The two theoretical curves plotted for $4.0 < E < 4.6$ GeV correspond to Figs. 5 and 7. The experimental points are taken from Refs. 2 and 6.

several simple (obvious, really) tests of the heavy-lepton proposal.

First, however, one potential difficulty must be surmounted. Below the heavy-lepton threshold there should exist a bound state of heavy leptons, so there is the possibility that a third spike in R should have been observed at ≈4.6 GeV. However, because $e^2/4\pi$ is so small the wave function of the heavy-lepton bound state is *extremely* small at the origin ($\psi_{LL}(0) \sim [(e^2/4\pi)m_L]^{3/2}$) so the spike actually subtends negligible area and could not have been seen.

A good feature of the heavy-lepton proposal is that it can be put to simple tests. Most models of heavy leptons[39,40] suggest that its purely leptonic decays will account for 0.4–0.5 of its width,

$$\frac{\Gamma(L\to\mu+\text{neutrinos})}{\Gamma(L\to\text{all})}\approx\frac{1}{5}-\frac{1}{4},$$
$$\frac{\Gamma(L\to e+\text{neutrinos})}{\Gamma(L\to\text{all})}\approx\frac{1}{5}-\frac{1}{4}. \tag{9.1}$$

These processes then imply small but measurable rates for μe + neutrinos and μ inclusive processes above 4.6–4.8 GeV. For example, choose $E = 6.0$ GeV where the heavy lepton contributes about $\frac{3}{4}$ unit to R. Then the percentage of events of the form μe + neutrinos, $P(e\mu)$, is roughly

$$P(e\mu)\approx(\tfrac{3}{4}/5)2(\tfrac{1}{5})(\tfrac{1}{4})$$
$$\approx 1\text{–}2\%. \tag{9.2}$$

Similarly, the probability of an event with a muon and anything else, $P(\mu X)$, is roughly

$$P(\mu X)\approx(\tfrac{3}{4}/5)2(\tfrac{1}{5})$$
$$\approx 5\%. \tag{9.3}$$

These two estimates give a good first test of the heavy muon possibility. Since there are other sources of μe and μX events, Eqs. (9.2) and (.3) should be treated as rough lower limits (assuming the heavy lepton has conventional properties[39,40]). In particular, leptonic decays of charmed mesons will add to these estimates, so there is the possibility that more elaborate tests than these will have to be passed before the existence of a heavy lepton is established. Of course, if the experimental μe and μ inclusive rates fall far below these estimates, then the heavy-lepton hypothesis is false.

Note added in proof. The discovery of sequential radiative transitions[41] of the $\psi'(3.7)$ to $\psi(3.1)$ considerably constrains the general theoretical framework discussed in the text. Assuming that these transitions proceed through the P states of charmonium,[41] we learn that the radiative transitions are much weaker than anticipated in the simplest charmonium models and the splitting between the P states is larger than anticipated. Taking the energies of the P states as input, the radiative widths of Eq. (7.4) are about 3 times too large.[41] Perhaps the overlap integrals in Eq. (7.4) are reduced by the mixing effects discussed in Sec. VII. The large P-state splittings mean that spin-dependent terms should not have been ignored in our coupled-channel models. These large effects are not understood and represent a real challenge to quark-model builders.

Several numerical challenges obviously remain for charmonium spectroscopists. One should calculate the rates $\psi'\to\gamma\gamma\psi$ and $\psi'\to\gamma\eta_c$ in a model with realistic D-D^* splitting to prove compatibility of the charm picture with the data.

ACKNOWLEDGMENT

The authors thank their colleagues at Cornell for many discussions. Particular thanks are due to K. Gottfried for help with the coupled-channel models, to M. Peskin for help with several of the potential model calculations, and to K. G. Wilson for several computer programs. Conversations with E. Eichten and K. Lane on ψ phenomenology and coupled-channel calculations are gratefully acknowledged.

*Work supported by the National Science Foundation.
†Work supported in part by the National Science Foundation under Grant No. GP-38863.

[1]J. J. Aubert *et al.*, Phys. Rev. Lett. 33, 1404 (1974); J.-E. Augustin *et al.*, *ibid.* 33, 1406 (1974); C. Bacci *et al.*, *ibid.* 33, 1408 (1974); G. S. Abrams *et al.*, *ibid.* 33, 1453 (1974).
[2]J.-E. Augustin *et al.*, Phys. Rev. Lett. 34, 764 (1975).
[3]We are using the term "charm" generically here. Later in the text it will refer specifically to the four-quark model of Ref. 5.
[4]M. Born and J. R. Oppenheimer, Ann. Phys. (Leipz.) 84, 457 (1927).
[5]J. D. Bjorken and S. L. Glashow, Phys. Lett. 11, 255 (1964); S. L. Glashow, I. Iliopoulous, and L. Maiani, Phys. Rev. D 2, 1285 (1970).
[6]G. 't Hooft, discussion comments at the Marseilles Conference on Gauge Theories, 1972 (unpublished); H. D. Politzer, Phys. Rev. Lett. 30, 1346 (1973); D. J. Gross and F. Wilczek, *ibid.* 30, 1343 (1973).
[7]E. Eichten *et al.*, Phys. Rev. Lett. 34, 369 (1975).
[8]H. Schnitzer, Brandeis report, 1974 (unpublished); J. S. Kang and H. J. Schnitzer, Phys. Rev. D 12, 841 (1975); C. G. Callen *et al.*, Phys. Rev. Lett. 34, (1975).
[9]R. Schwitters, invited talk at the Washington meeting of the American Physical Society, 1975 (unpublished).
[10]T. Appelquist and H. Georgi, Phys. Rev. D 8, 4000 (1973); A. Zee, *ibid.* 8, 4038 (1973).
[11]Theories with more than four quarks have been considered recently by R. M. Barnett [Phys. Rev. Lett. 34, 41 (1975)], H. Harari [Phys. Lett. 57B, 265 (1975)] and F. Wilczek [Princeton report, 1975 (unpublished)].
[12]Private communication from H. Harari and J. D. Bjorken.
[13]B. Harrington, S. Y. Park, and A. Yildiz, Phys. Rev. Lett. 34, 168 (1975); 34, 706 (1975).
[14]J. Kogut and L. Susskind, Phys. Rev. D 9, 3501 (1974); K. Wilson, *ibid.* 10, 2445 (1974).
[15]R. Hofstadter, invited talk at the Washington meeting of the American Physical Society, 1975 (unpublished).
[16]J. Kogut and L. Susskind, Phys. Rev. Lett. 34, 767 (1975).
[17]H. Fritzsch, M. Gell-Mann, and H. Leutwyler, Phys. Lett. B 47B, 365 (1973).
[18]H. Georgi and S. L. Glashow, Phys. Rev. Lett. 32, 438 (1974); S. Weinberg, *ibid.* 31, 494 (1973).
[19]This discussion appears in *Principles of the Theory of Solids* by J. M. Ziman (Cambridge Univ. Press, London, 1964).
[20]Leonard I. Schiff, *Quantum Mechanics* (McGraw-Hill, New York, 1955).
[21]J. Schwinger, Phys. Rev. 128, 2425 (1962).
[22]Equivalent-boson methods for the massive Schwinger model were first obtained by J. Kogut and L. Susskind, Phys. Rev. D 11, 3594 (1975).
[23]A. Casher, J. Kogut, and L. Susskind, Phys. Rev. Lett. 31, 792 (1973); Phys. Rev. D 10, 732 (1974).
[24]In $(1+1)$-dimensional models of confinement the term "charge" denotes quark number. In a non-Abelian gauge theory of confinement, "charge" would be replaced by "color."
[25]An important ingredient in the proof of confinement for the massive Schwinger model is that scalar field configurations with asymmetric boundary conditions $[\phi(z=+\infty, t) \neq \phi(z=-\infty, t)]$ require infinite energy. See Ref. 22.
[26]Jürg Fröhlich, Phys. Rev. Lett. 34, 833 (1975).
[27]See, for example, S. Borchardt, V. S. Mathur, and S. Okubo, Phys. Rev. Lett. 34, 38 (1975), and A. De Rújula, H. Georgi, and S. L. Glashow, Phys. Rev. D 12, 147 (1975).
[28]The authors thank M. Peskin for the explicit expression for $\psi(0)$ in terms of Airy functions Ai and Bi.
[29]T. Appelquist and H. D. Politzer, Phys. Rev. D 12, 1404 (1975).
[30]The term "virtual bound state" is discussed and defined precisely in *Introductory Nuclear Theory* by L. R. B. Elton (Saunders, Philadelphia, 1966).
[31]T. Appelquist and D. H. Politzer, Phys. Rev. Lett. 34, 43 (1975) (these authors predicted charmonium states and stressed the importance of asymptotic freedom in the determination of their properties); A. De Rújula and S. L. Glashow, Phys. Rev. Lett. 34, 46 (1975).
[32]Y. Nambu, lectures presented at the Copenhagen Summer Symposium, 1970 (unpublished); L. Susskind, Nuovo Cimento 69A, 457 (1970). More recently, P. Goddard *et al.*, Nucl. Phys. B56, 109 (1973).
[33]We thank K. Gottfried for the solution of the coupled-channel problem.
[34]K. Gottfried, in *Elementary Particle Physics and Scattering Theory*, 1967 Brandeis Institute in Theoretical Physics, edited by M. Chrêtien and S. S. Schweber (Gordon and Breach, New York, 1970), Vol. II; H. Feshbach, Ann. Phys. (N.Y.) 5, 357 (1958).
[35]We thank M. Peskin for obtaining the Green's function G_- analytically for wedge-shaped potentials. This calculation was one of several checks on the computer solution of the coupled-channel problem.
[36]T. Appelquist, A. De Rújula, H. D. Politzer, and S. L. Glashow, Phys. Rev. Lett. 34, 365 (1974). This article discusses charmonium spectroscopy without a commitment to a specific model.
[37]The notation D, D^*, etc. follows that in the article by M. K. Gaillard, B. W. Lee, and J. L. Rosner, Rev. Mod. Phys. 47, 277 (1975).
[38]G. Zweig, CERN Report No. TH402, 1964 (unpublished).
[39]Y.-S. Tsai, Phys. Rev. D 4, 2821 (1971).
[40]J. D. Bjorken and C. H. Llewellyn Smith, Phys. Rev. D 7, 887 (1973).
[41]W. Braunschweig *et al.*, Phys. Lett. 57B, 407 (1975).